



Feasibility Assessment of Synchronous Operations of the North American Eastern and Western Interconnections

Final Project Report

S-92G

Power Systems Engineering Research Center
*Empowering Minds to Engineer
the Future Electric Energy System*



Feasibility Assessment of Synchronous Operations of the North American Eastern and Western Interconnections

Final Project Report

Project Team

Thomas J. Overbye, Project Leader

Komal S. Shetye

Texas A&M University

Graduate Students

Hanyue Li

Wei Trinh

Jessica Wert

Texas A&M University

PSERC Publication 21-02

January 2021

For information about this project, contact:

Thomas J. Overbye
Texas A&M University
Department of Electrical and Computer Engineering
308C, Wisenbaker Engineering Building
College Station, Texas 77843-3128
Phone: 979-458-5001
Email: overbye@tamu.edu

Power Systems Engineering Research Center

The Power Systems Engineering Research Center (PSERC) is a multi-university Center conducting research on challenges facing the electric power industry and educating the next generation of power engineers. More information about PSERC can be found at the Center's website: <http://www.pserc.org>.

For additional information, contact:

Power Systems Engineering Research Center
Arizona State University
527 Engineering Research Center
Tempe, Arizona 85287-5706
Phone: 480-965-1643
Fax: 480-727-2052

Notice Concerning Copyright Material

PSERC members are given permission to copy without fee all or part of this publication for internal use if appropriate attribution is given to this document as the source material. This report is available for downloading from the PSERC website.

© 2021 Texas A&M University. All rights reserved.

Acknowledgements

This is the final report for the Power Systems Engineering Research Center (PSERC) research project titled “Feasibility Assessment of Synchronous Operations of the North American Eastern and Western Interconnections” (S-92G). We express our appreciation for the support provided by PSERC’s industry advisors and HVDC Owner/Operators¹:

- Sirisha Tanneeru¹ (Xcel Energy)
- Bradley Curtis, Casey Cathey, Charles Cates, Chase Harrod, Douglas Bowman, Harvey Scribner, Jay Caspary (Retired), Jim Gonzalez, Jonathan Hayes, Scott Jordan (Southwest Power Pool)
- Chris Pink, Christopher Gilden, Cody Sickler, Ryan Hubbard (Tri-State Generation and Transmission)
- Garrick Nelson, Gayle Nansel, James Hirning, Rebecca Johnson, Roy Gearhart (Western Area Power Administration)

The industry advisors would like to recognize the PSERC Researchers at Texas A&M University, Tom Overbye, Komal Shetye, Hanyue Li, Wei Trinh, and Jess Wert for their extra efforts to perform this study and advance power flow and dynamic simulation algorithms, while taking on the extra challenges required to educate the next generation of scientists and engineers during this unusual year of COVID 19.

Executive Summary

Most of the electricity used in North America is supplied by four major interconnects, each operating at 60 Hz but asynchronous with each other. These interconnects are the Eastern (EI), the Western (WI), Texas (ERCOT), and the Quebec Interconnection. All of these ac networks are internally synchronized, and are linked to each other only through dc ties. So far, interconnection studies have mainly focused on the economic or resource planning aspects or the use of HVDC for transmission expansion and design. A key area of improvement mentioned in these studies has been contingency and stability analyses. The feasibility of ac tie connection has been studied less frequently, with the need for improved assessments considering automatic generation control (AGC) in long-term dynamics identified in literature. System dynamics is a key concern while considering operating two large grids synchronously.

With this in view, the overall goal of this project is to consider the dynamic aspects of an ac interconnection of the North American Eastern and Western Interconnection (EI and WI) grids. However, since much of the information about these actual grids is considered critical energy infrastructure information (CEII) and hence its publication is restricted, realistic but fictitious synthetic grids are used to demonstrate the methodology. These grids cover the same geographic footprints as the real ones, use real generation information since it is publicly available and mimic load distribution from census data, but the transmission lines are entirely fictitious.

The methodology involves first overcoming challenges associated with combining actual detailed WECC and EI models and second making the actual connections between the synthetic east and west systems with ac ties, which collectively form the “Interface”. Challenges include the ability to handle very large systems with overlapping bus and area numbers; determining the location, number and types of connections needed for reasonable steady state and dynamic performance of the combined system; initializing tie flows for studies, etc. Then after assigning appropriate impedances and ratings, a few static power flow studies are performed to determine distribution of flows across each tie, and estimate the MW transfer capability. The goal of these studies is to demonstrate methods to pinpoint the heavier loaded ties and locations where modest upgrades could lead to major improvement in transfer capability.

Next, the main part of the project i.e. dynamic assessments of the interconnection involves a wide variety of dynamic simulations of the systems. The key limiting characteristic on interconnecting the EI and WI is that during generator loss contingencies in the WI, approximately 75 to 80% of the lost power will flow through the Interface from east to west. This is due to the governor response that takes place uniformly through the interconnect and most of the generation is east of the Interface. This issue is fundamental to interconnecting large grids and does require any interface joining two such larger grids be able to handle this flow (at least until AGC can respond). In particular for the EI and WECC, there need to be more than just a few tielines. For the flow to return to pre-contingency values, AGC needs to be modeled in these simulations, which is not a common practice. To address this, AGC is implemented and included in our dynamic simulations run for several minutes. In the scenarios run both for the real and synthetic interconnections, the grids are stable when AGC response is considered.

A major challenge associated with these analyses is understanding what is occurring in the large scale electric grids, particularly when they could be subject to unusual operating conditions such as those associated with a new ac interconnection. This in addition to the large quantity of simulation results, especially dynamics with hundreds of thousands of buses, models, states, etc. To this end, geographic data views (GDV), which are electric grid display objects whose location is dynamically determined from geographic information embedded in an electric grid model, are developed and used extensively. Different examples of GDV's and how they can meaningfully convey a large amount of key information are shown.

The studies shown in this report are not meant to be all-encompassing and covering all possible conditions and scenarios. Rather, these are preliminary studies performed to illustrate issues associated with the interconnection of large-scale grids with an eye towards providing a test system for other researchers. These grids i.e. the individual synthetic east and west and their ac interconnected versions are available publicly for researchers (electricgrids.tamu.edu) to access and run their own scenarios in addition to those shown in this report. This may include, 1) different ac tie connections, 2) static and dynamic contingency scenarios, 3) loading conditions, 4) renewable generation, 5) time series simulations such as those used in OPFs, and so on.

Project Publications:

- [1] Thomas J. Overbye, Jessica L. Wert, Komal S. Shetye, Farnaz Safdarian, Adam B. Birchfield, "The Use of Geographic Data Views to Help With Wide-Area Electric Grid Situational Awareness," Submitted to *Texas Power and Energy Conference (TPEC) 2021*, Feb. 2021, College Station, TX.
- [2] Komal S. Shetye, Thomas J. Overbye, Hanyue Li, Julian Thekkemathote, "Considerations for Interconnection of Large Power Grid Networks," Submitted to *Power and Energy Conference at Illinois (PECI) 2021*, Apr. 2021, Champaign, IL.
- [3] Thomas J. Overbye, Komal S. Shetye, Jessica L. Wert, Wei Trinh, Tracy Rolstad, Jamie Weber, "Techniques for Maintaining Situational Awareness During Large-Scale Electric Grid Simulations," Submitted to *Power and Energy Conference at Illinois (PECI) 2021*, Apr. 2021, Champaign, IL.

Table of Contents

1. Introduction.....	1
1.1 Background and Literature Review	1
1.2 Overview of the Problem.....	2
1.3 Report Organization	2
2. Eastern and Western Electric Grid Networks, Real and Synthetic.....	4
2.1 Real EI and WI Grids Overview	4
2.2 Synthetic East and West Grids Introduced.....	6
2.3 Synthetic East and West Grids Interconnected	8
2.4 Interface Flow Characteristics and Capacity	10
2.4.1 Power Transfer Distribution Factor Analysis	10
2.4.2 Available Transfer Capability Analysis.....	11
2.4.3 MW Transfers with AC Power Flow	12
3. Dynamics	13
3.1 Introduction	13
3.2 Actual Electric Grid Results Summary	13
3.3 Long-term AGC Modeling.....	15
3.4 Synthetic Grid Simulation Results	17
4. Geographic Data Views for Wide-Area Visualization	24
4.1 Introduction	24
4.2 Geographic Data Views.....	25
4.3 Use of Layout Algorithms	28
4.4 GDV Summary Objects.....	30
5. Concluding Remarks.....	32
References.....	34

List of Figures

Figure 1.1 North American Electric Interconnects (Source NERC).....	1
Figure 2.1 Generation for the Heavy Loading Scenario.....	5
Figure 2.2 Generation for the Light Loading Scenario.....	5
Figure 2.3 Overview Visualization of the Combined Grids	6
Figure 2.4 Synthetic Western (SW) US Grid Oneline.....	7
Figure 2.5 Synthetic Eastern (SE) US Grid Oneline.....	7
Figure 2.6 Synthetic Eastern and Western US grids with the Onelines meeting at the Red Boundary and the Seven Transmission Lines and Transformers in the Interface Shown in Magenta.....	9
Figure 2.7 PTDFs of AC Ties for Different Transfer Scenarios.....	11
Figure 3.1 MW Flows on the EI-WI Interface.....	14
Figure 3.2 WECC Bus Frequencies as Thin (Thick) Lines for Separate (Combined) Systems ...	15
Figure 3.3 Frequency Variation at All Substations for a WECC Generator Loss Contingency...	15
Figure 3.4 Initial AGC Response Simulation with a 0.08 Hz Oscillation	17
Figure 3.5 Modified System AGC Response.....	17
Figure 3.6 Interface Flow MW (West to East Positive) Over 30 Seconds	18
Figure 3.7 Frequency Response at Ten Buses in the West Over 30 Seconds.....	19
Figure 3.8 Voltage Magnitude Response at Ten Buses in the West Over 30 Seconds.....	19
Figure 3.9 Interface Flow MW (West to East Positive) Over 120 Seconds	20
Figure 3.10 Frequency Response at Ten Buses in the West Over 120 Seconds.....	20
Figure 3.11 Voltage Magnitude Response at Ten Buses in the West Over 120 Seconds.....	21
Figure 3.12 Voltage Magnitude Deviation at Ten Buses in the West Over 120 Seconds	21
Figure 3.13 Frequency Response at All 80,000 Buses	22
Figure 3.14 Voltage Magnitude Deviation at All 80,000 Buses.....	23
Figure 3.15 Visualization of System at Ten Seconds Using Voltage Contour and GDV Summary Objects.....	23
Figure 4.1 82,000 Bus System Oneline	26
Figure 4.2 82,000 Bus System Area GDVs	26
Figure 4.3 82,000 Bus Grid Substation GDVs	29
Figure 4.4 82,000 Bus Substation GDVs with Layout	29
Figure 4.5 82K System Generation Summary Objects using a 25 by 15 Grid	30
Figure 4.6 82K Substation Flow Visualization with Aggregate Line Flows (16 by 8 Grid).....	31

Figure 4.7 82K Substation Flow Visualization with Aggregate Line Flows (28 by 16 Grid)..... 31

List of Tables

Table 2.1 Synthetic Networks Summary	8
Table 2.2 AC Ties Summary	9
Table 2.3 AC Ties Initial Flows.....	10
Table 2.4 PTDF Analysis Results.....	11

1. Introduction

1.1 Background and Literature Review

Most of the electricity used in North America (NA) is supplied by four major interconnects, shown in Figure 1.1, with each operating at 60 Hz but asynchronous with each other. These interconnects are the Eastern (EI), the Western (WI), Texas (ERCOT), and the Quebec Interconnection. All of these ac networks are internally synchronized and are linked to each other only through dc ties. However, for several years between 1967 and the early 1970's the EI and WI were operated as a single synchronous system [1], which included 94% of the US generating capacity [2]. This interconnection was motivated by the November 1965 Northeast Blackout, which left 30 million people without power across eleven US states, and Canada. The interties functioned well at first but soon became unstable due to oscillations on the western side and large inadvertent exchanges. This led to overloading of transmission facilities, major system breakups, and reduced transmission capacity. Interconnecting large grids especially with ac ties is a big challenge that needs rigorous assessment and planning.

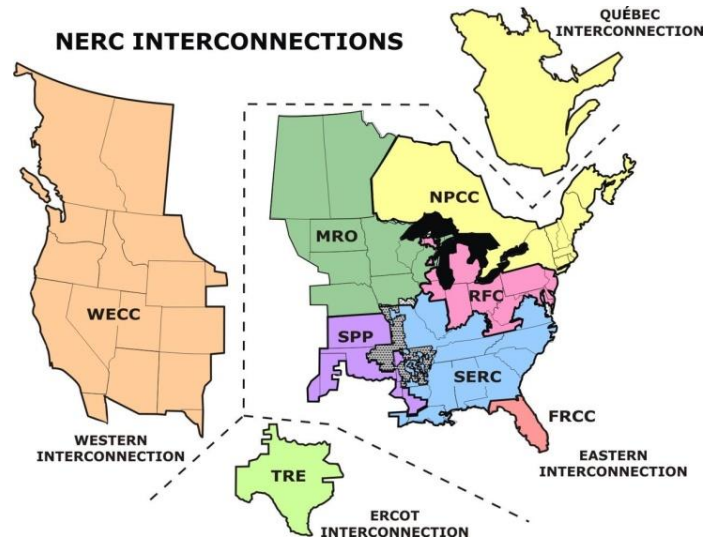


Figure 1.1 North American Electric Interconnects (Source NERC)

There have been several studies and implementations around the world of joining large grids with dc ties, and some examples with ac ties. In 1991, the continental Europe grid was broken into two synchronous grids separating western and central Europe due to political issues, and reconnected in 2000 with the emergence of favorable conditions [3]. This was done after extensive steady-state and dynamics studies [4]. For further expansion, [5] studied the feasibility of connecting this synchronous grid with the Baltic States. This involved creating a merged static and dynamic model of the two grids. Some of the issues found in this process were the emergence of very low frequency (~ 0.07 Hz) oscillations, as well as transfer capability limitations due to local congestion. Reference [6] considered possible scenarios for interconnecting Korea and Japan using 765 kV HVAC within the Korean peninsula and 180 kV HVDC interconnection between the islands. Results of power flow studies for load increase

scenarios for the ac ties and different power injections for dc were shown. The need for, political issues with, and advantages of both schemes were discussed. In [7], two candidates were evaluated for the future Chinese “super grid”, to enable bulk capacity long distance power transmission, i.e. 1) the ultra-high-voltage ac (UHVAC) synchronous power grid, 2) the extra high-voltage ac (EHVAC) asynchronous super power grid. This paper provided qualitative assessments of both schemes considering security, economic, and environmental factors based on which the EHVAC asynchronous method was found to be superior, with a caveat that additional studies are needed to verify the results. The benefits of the ac connections were lower short circuit currents compared to the asynchronous system, while the main disadvantage was the susceptibility to cascading failures.

In NA, the more recent as well as previous interconnection studies have mainly focused on the economic or resource planning aspects [8], [9] or the use of HVDC for transmission expansion and design [10]. These works are part of a larger effort comprising of research and industry members that proposed four different high-capacity wide-area transmission infrastructure designs to expand the US grid [11]. This study was focused on leveraging dc systems i.e. upgrading the existing back-to-back (B2B) dc ties and/or building long HVDC lines or overlays. While this included rigorous analyses considering future capacity, carbon policies, etc., a key area of improvement mentioned in [11] is performing contingency and stability analyses. The feasibility of ac tie connection has been studied less frequently [12], with the need for more up-to-date assessments with improved models such as automatic generation control (AGC) modeling in long-term dynamics, etc. identified in both [12] and [13]. System dynamics is a key concern while considering operating two large grids synchronously.

1.2 Overview of the Problem

The overall goal of this project is to consider the dynamic aspects of an ac interconnection of actual North American Eastern and Western Interconnection grids. However, since much of the information about these actual grids is considered critical energy infrastructure information (CEII) and hence its publication is restricted, the project also considers the dynamic interconnection of two large-scale synthetic grids [14], [15] with further information about all of these grids provided later in this report. A more detailed report that contains CEII has been provided to the PSERC member company sponsoring this project (i.e., SPP). This report uses the synthetic grids and discusses issues such as modeling two different interconnections that use different software packages, actual ac connection of the grids at different locations, long-term dynamics and AGC modeling, wide-area visualization, etc. PowerWorld Simulator Version 22 is used for all the simulation results shown in this report due to its ability to model very large bus numbers, and represent the dynamic models of both the EI and WI grids that usually originate from different software packages. The report present results of both the actual EI and WI systems interconnected, and the synthetic interconnected system. A key reason behind this is to show the impact of system loading on dynamics; heavy and light load condition cases were available for the real systems but the synthetic US grid used currently reflects peak load conditions only.

1.3 Report Organization

The report is organized as follows. Chapter 2 describes a description of the studied electric grids and provides some static (power flow and contingency analysis results). Chapter 3 considers the

dynamic aspects of the grids. Since understanding the overall behavior of these large-scale systems was a key concern, Chapter 4 provides new visualization concepts that were developed, in part, as a result of this project. The last chapter provides the conclusions.

2. Eastern and Western Electric Grid Networks, Real and Synthetic

2.1 Real EI and WI Grids Overview

The project commenced with all the team members signing the necessary NDAs to obtain access to the actual power flow and dynamics models associated with the EI and WI grids. Two different base case conditions are considered, one representing a heavy loading scenario and one representing a light loading scenario. The cases for the WI were obtained from Western Electricity Coordinating Council (WECC) in the PowerWorld Simulator power flow and stability model *.pwb format while the cases for the EI were obtained from SPP in the Siemens Power Technologies International (Siemens PTI) transmission planning and analysis software PSS@E format. All of the buses were assigned to substations and the substations were geo-mapped. Since these cases had overlapping numbers (e.g., for the buses) the numbers in the WI were modified with the bus numbers increased by 2,000,000, and the area and zone numbers increased by 2000. An item to note here is that the underlying simulation software should be able to model such large bus numbers, which is not the case with all software packages but was not an issue with the packaged used here for analysis. The grids were then combined using nine ac connections determined jointly with SPP. Collectively this set of tie lines joining the two grids will be known as “the Interface.” Overall, each grid had approximately 110,000 buses with the heavy case having about 848 GW of generation and 828 GW of load while the light load case had 419 GW of generation and 408 GW of load .

Since all of the grid devices had associated geographic locations, a wide variety of difference visualizations were used through the project with many based on the geographic data view (GDV) approach of [39] (with further details given in Chapter 4). As an example, Figure 2.1 shows the substation generation for the heavy loading scenario with the size of each oval proportional to the substation generation and the substations with more generation shaded darker blue. Figure 2.2 shows a similar display for the light loading scenario, with a difference that now some ovals are shaded red to indicate negative generation due to pumped hydro. Figure 2.3 shows a high level transmission view of the combined grids with the different colors used to indicate different nominal voltage levels (green for above 700 kV, orange for 500 kV, and red for 345 kV). In the figure, the substations close to the Interface are highlighted.

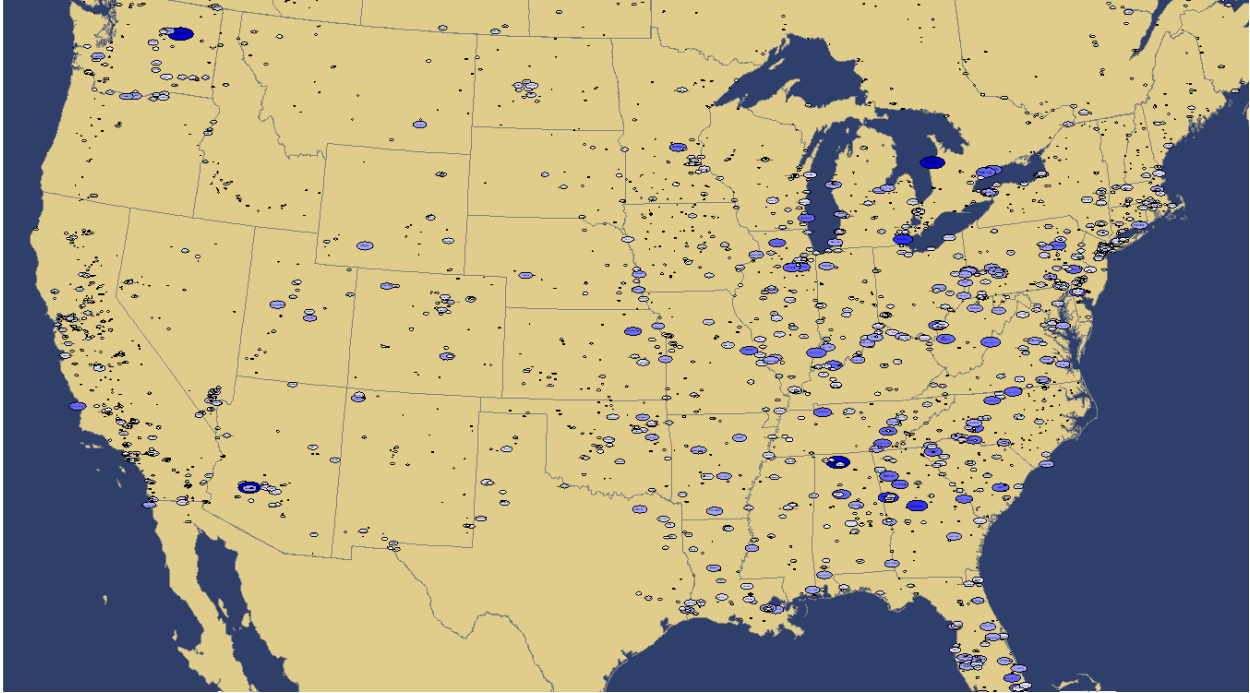


Figure 2.1 Generation for the Heavy Loading Scenario

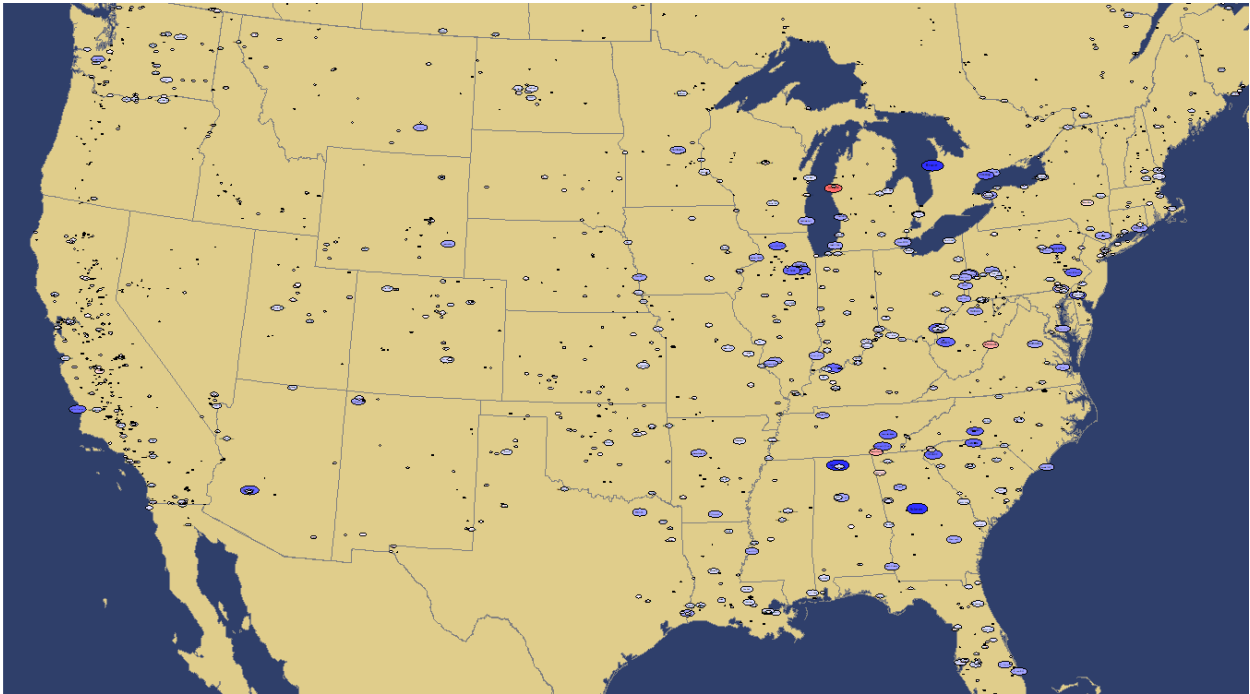


Figure 2.2 Generation for the Light Loading Scenario

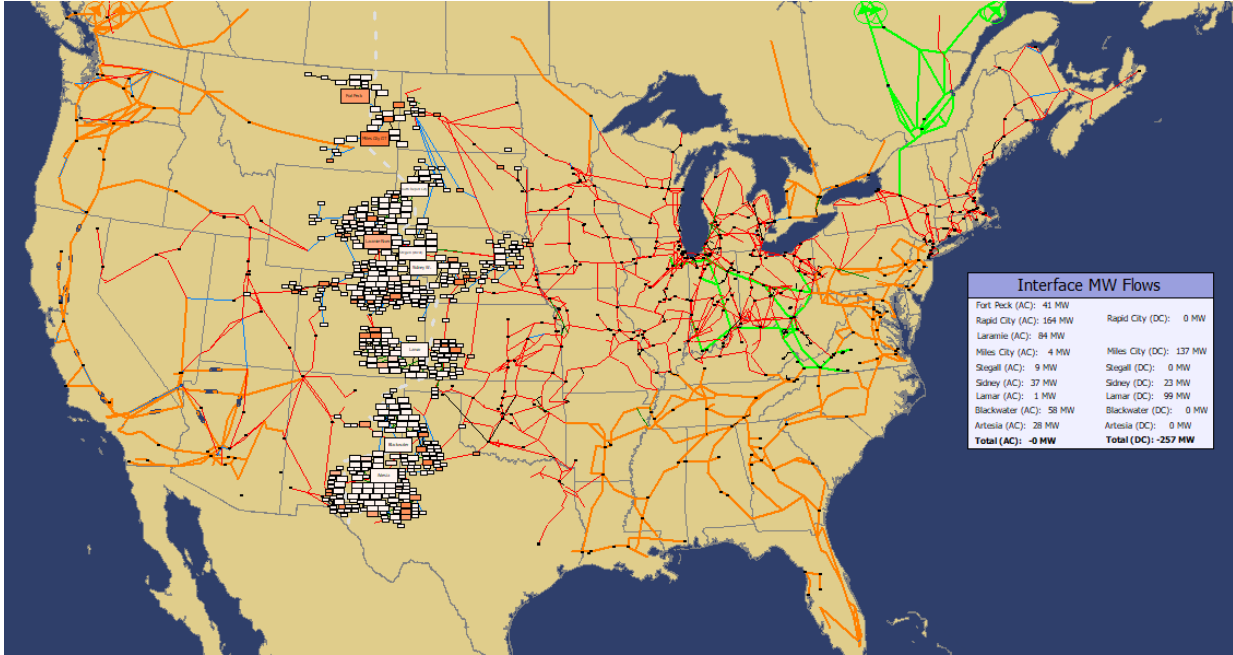


Figure 2.3 Overview Visualization of the Combined Grids

2.2 Synthetic East and West Grids Introduced

As mentioned earlier, using realistic synthetic grids allows us to present research results without revealing critical energy infrastructure information (CEII). Accordingly, the project uses two synthetic grids [14], [15], available at [16], geographically located over the EI and WI footprints. The 70,000-bus eastern synthetic grid and the 10,000-bus western case bear no relation to the actual grids except that generation and load profiles are similar, based on public data. The transmission lines are fictitious. These test systems are meant to reflect heavy load, i.e. peak summer conditions. The areas in each of these grids are named in reference to US state names, where each area covers the footprint of an entire state or a portion of it (e.g. Chicago Northern Illinois).

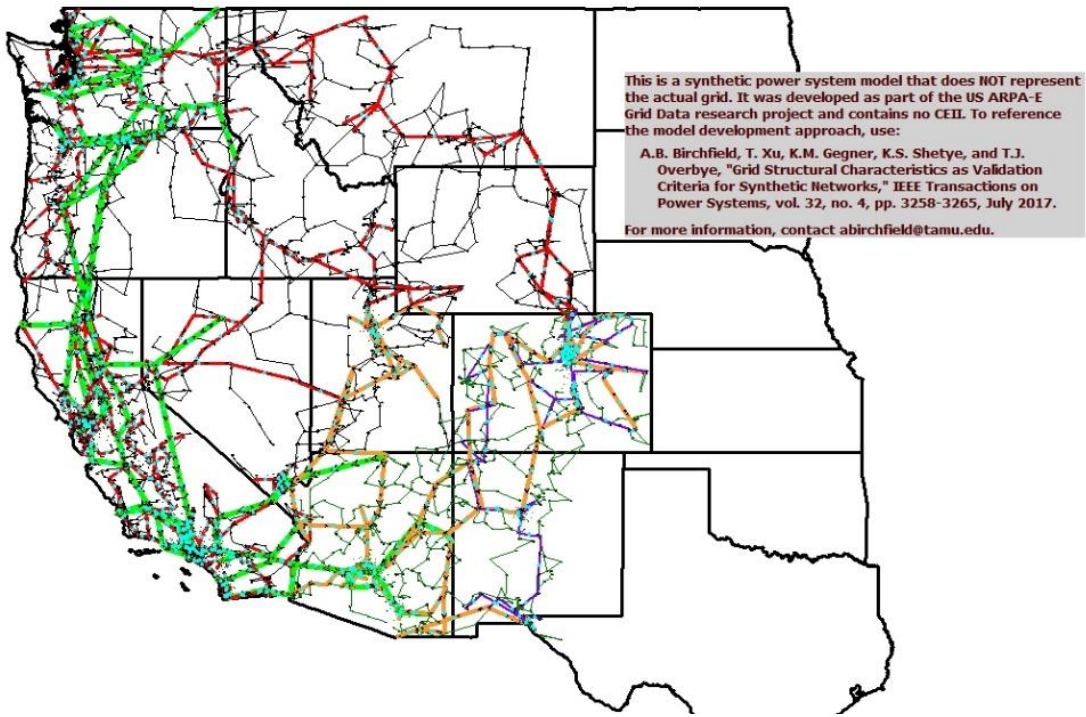


Figure 2.4 Synthetic Western (SW) US Grid Online

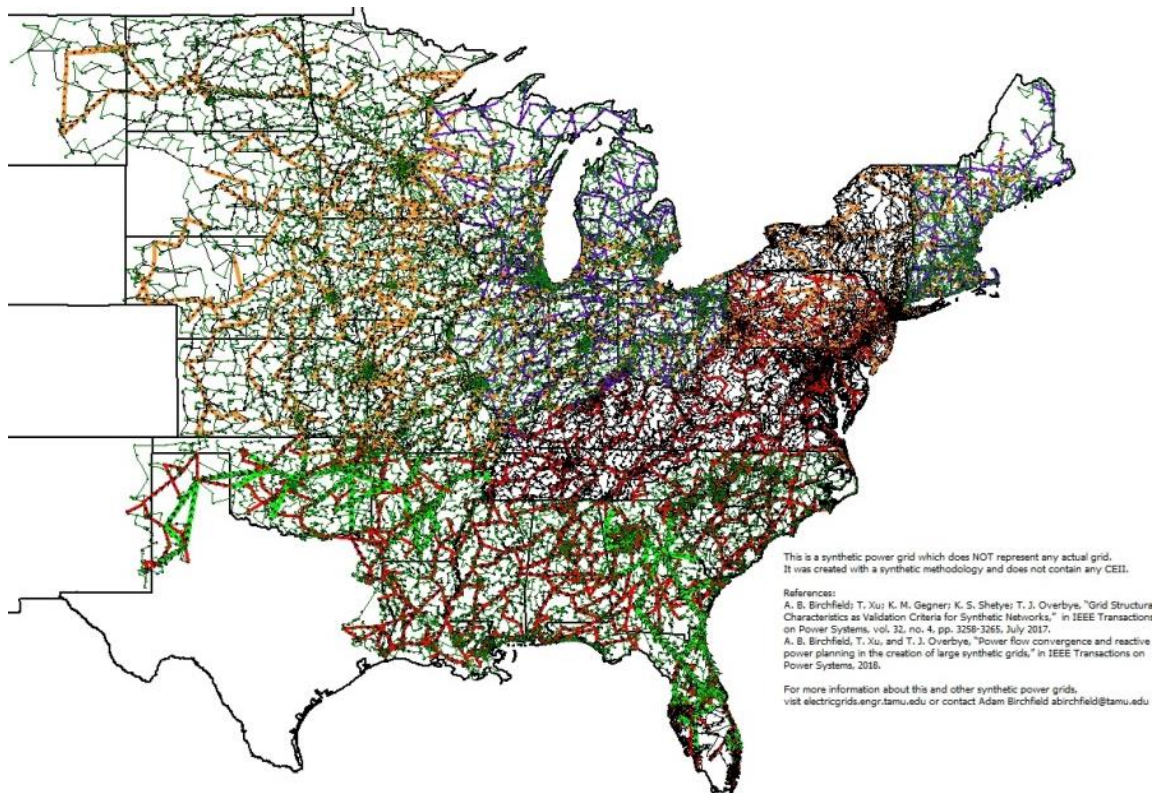


Figure 2.5 Synthetic Eastern (SE) US Grid Online

Table 2.1 Synthetic Networks Summary

Property	Synthetic East (SE)	Synthetic West (SW)
# of Buses	70,000	10,000
# of Gens	10,390	2,485
# of Loads	38,180	4900
# of Lines	71,353	9726
Total Gen (MW)	613,000	15,400
Total Load (MW)	594,700	151,000
# of Areas	52	16
Voltage Levels (kV)	13-24, 69, 100, 115, 138, 161, 230, 345, 500, 765	13-24, 115, 138, 161, 230, 345, 500, 765

2.3 Synthetic East and West Grids Interconnected

Naturally, geographic proximity of two buses/substations, one in each system, is one of the main factors in deciding the points of interconnection. If they are at the same nominal voltage level, they can be connected by jumpers or what are also called zero impedance branches. Otherwise, connections can be made with transformers, which would be more expensive. Another important aspect of choosing the connection points and locations is the transmission infrastructure around it. Assuming that these ac ties are meant to support sizeable transactions, the lines immediately connecting these ties to the rest of the SE and SW on each side should be able to handle the flows. This would be the minimum cost approach. Else, the interconnection plan needs to include rating upgrades or construction plans near the ties.

The number of connection points depends on factors such as the desired MW transfer capacity. Having too few lines would prevent maximizing this capability, potentially causing congestion, in addition to weakening the connection between two large systems, from both a steady state and dynamics perspective. A major motivation, especially relevant in the US is to assess the potential for improved generation (mostly renewable) resource utilization, e.g. the benefits of trying to connect the wind centers in the middle of the US to the load centers in the West.

Considering all this, seven transmission line and transformer connections were made between SW and SE systems, numbered in Figure 2.6:

- 1) Glasgow (Montana) to Fort Peck (Montana)
- 2) Hardin (Montana) to Colstrip (Montana)
- 3) Wheatland (Wyoming) to Scottsbluff (Nebraska)
- 4) Peetz (Colorado) to Sidney (Nebraska)
- 5) New Raymer (Colorado) to Kimball (Nebraska)
- 6) Burlington (Colorado) to Goodland (Kansas)
- 7) Lamar (Colorado) to Johnson (Kansas)

Note that unlike the real EI and WI cases, there were no pre-existing dc ties at their interface or added during this study. Using the same notation as was with actual grid model, collectively these lines and transformers will also be known as “the Interface.”

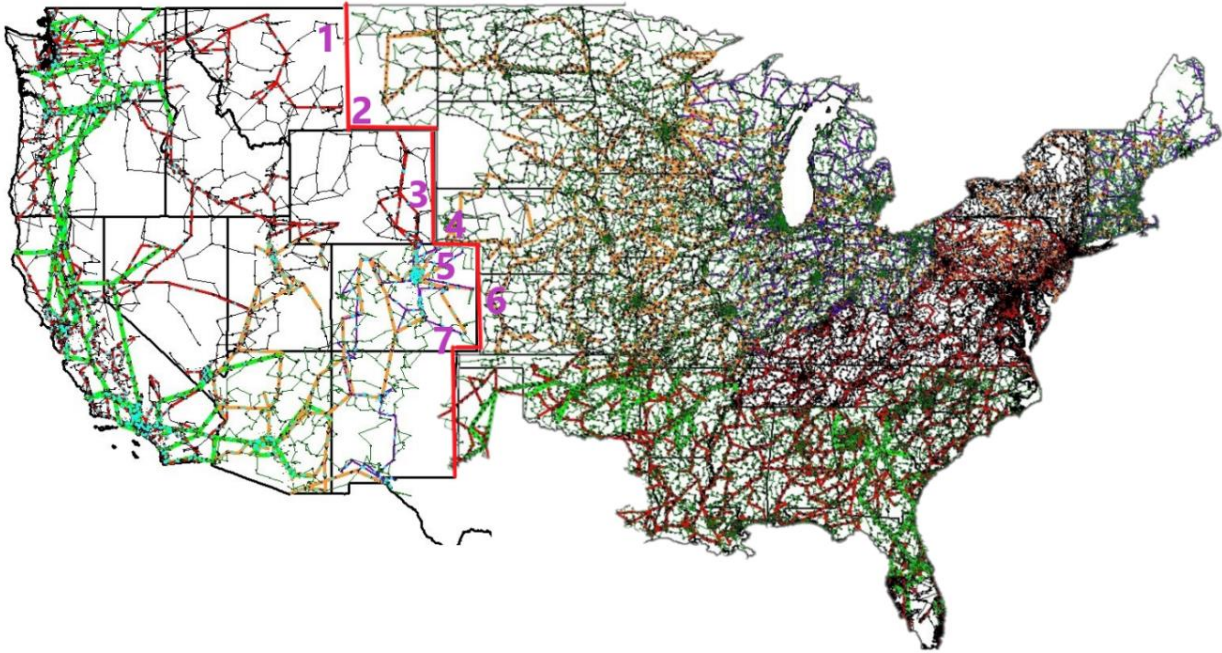


Figure 2.6 Synthetic Eastern and Western US grids with the Onelines meeting at the Red Boundary and the Seven Transmission Lines and Transformers in the Interface Shown in Magenta

A key task then is to assign appropriate impedance values and MVA ratings (i.e. limits) to these newly created ties. Zero impedance branches are commonly modeled in the power flow as very low reactance branches; this approach was followed here. Ratings were assigned based on those of nearby branches, choosing the lower end in case of a large difference for a transformer.

Table 2.2 AC Ties Summary

No.	From Bus (kV)	To Bus (kV)	X (p.u.)	Lim (MVA)
1	Glasgow (138)	Fort Peck (500)	0.055	600
2	Hardin (345)	Colstrip (500)	0.06	1200
3	Wheatland (345)	Scottsbluff (500)	0.07	1400
4	Peetz (500)	Sidney (500)	0.03	2000
5	New Raymer (500)	Kimball (500)	0.02	2000
6	Burlington (500)	Goodland (500)	0.03	2000
7	Lamar (500)	Johnson (161)	0.04	800

It is expected that such interconnections would be extensively used to assess the transfer capacity between two existing system. For such studies, it is important to initialize the flows on these newly created ac ties ideally or close to 0 MW. Note that some flows may be unavoidable due to the difference in the power sharing among areas and generators on either side due to system-specific participation factors. Hence, the focus can or should be on ensuring that the Net MW flows on the ac ties is nearly zero. In this particular case, this involved changing the dispatch of certain generators on the WI side given that the slack bus generator was in the SE.

Table 2.3 AC Ties Initial Flows

From Name	To Name	Branch Device Type	MW From
HARDIN	COLSTRIP	Transformer	-196.4
BURLINGTON	GOODLAND	Line	-119.2
LAMAR	JOHNSON	Transformer	-100.5
NEW RAYMER	KIMBALL	Line	36.1
PEETZ	SIDNEY	Line	41.4
GLASGOW	FORT PECK	Transformer	57
WHEATLAND	SCOTTSBLUFF	Transformer	273.6
Total MW			-8.0

2.4 Interface Flow Characteristics and Capacity

This part discusses power flow results of the expected flows across the Interface and its potential transfer capacity. This involves methods such as power transfer distribution factors (PTDFs) to understand flow patterns on the Interface ties, available transfer capability (ATC) calculations using dc power flow to find the maximum transfer possible under different scenarios, and maximum possible MW transfers in each direction across the Interface considering a full ac power flow solution. The goal here is to show the methodology behind estimating the capacity of such connections and planning for potential upgrades.

2.4.1 Power Transfer Distribution Factor Analysis

PTDFs show the percentage of the transfer that will flow on each element (i.e. a transmission line or a transformer branch) for a transaction between a defined source (buyer) and sink (seller). Here, the buyers and sellers are on opposite sides of the Interface, so 100% of the transfer goes through the Interface. For six transfer scenarios, PTDFs were calculated for the whole system including the ac ties using a linearized lossless dc power flow solution. Table 2.4 shows the PTDFs on the ties for the six transfer scenarios that are between either 1) two subsystems such as the whole of the Synthetic East and West grids, or 2) Areas in each grid. Here NE: Nebraska, CO: Colorado, MT: Montana, MN: Minnesota, NM: New Mexico, OK: Oklahoma, SD: South Dakota, ID: Idaho, AZ: Arizona, and IL: Illinois.

Table 2.4 and Figure 2.7 show that for a given transfer across the Interface, one can expect a flow of at most 25% through any one of the ties, with around 5% on the lower side. In most transfer scenarios, a major portion of the flows would occur through the Hardin-Colstrip and the Burlington-Goodland ties, i.e. around a fifth to a quarter each, of the total MW transferred. These would be followed by the New Raymer-Kimball and the Peetz-Sidney ties. On the other hand, Fort Peck is expected to carry at most 6% of any transfer.

Table 2.4 PTDF Analysis Results

No.	PTDF From Bus	PTDF To Bus	Buyer to Seller, PTDF (%)						Avg.
			Whole SE to SW	NE to CO	MT to MN North	NM to OK	SD to ID	AZ to IL North	
1	Glasgow	Fort Peck	5.88	3.16	8.41	4.56	7.19	5.42	5.77
2	Hardin	Colstrip	20.95	12.78	38.3	17.07	25.03	19.93	22.34
3	Wheatland	Scottsbluff	8.4	7.8	11.06	7.67	8.66	7.92	8.58
4	Peetz	Sidney	13.23	16.94	8.71	15.15	13.05	13.78	13.47
5	New Raymer	Kimball	17.04	21.5	11.61	18.16	17.77	17.81	17.32
6	Burlington	Goodland	22.87	26.03	14.89	25.17	19.2	23.35	21.92
7	Lamar	Johnson	11.63	11.79	7.03	13.22	9.1	11.79	10.76

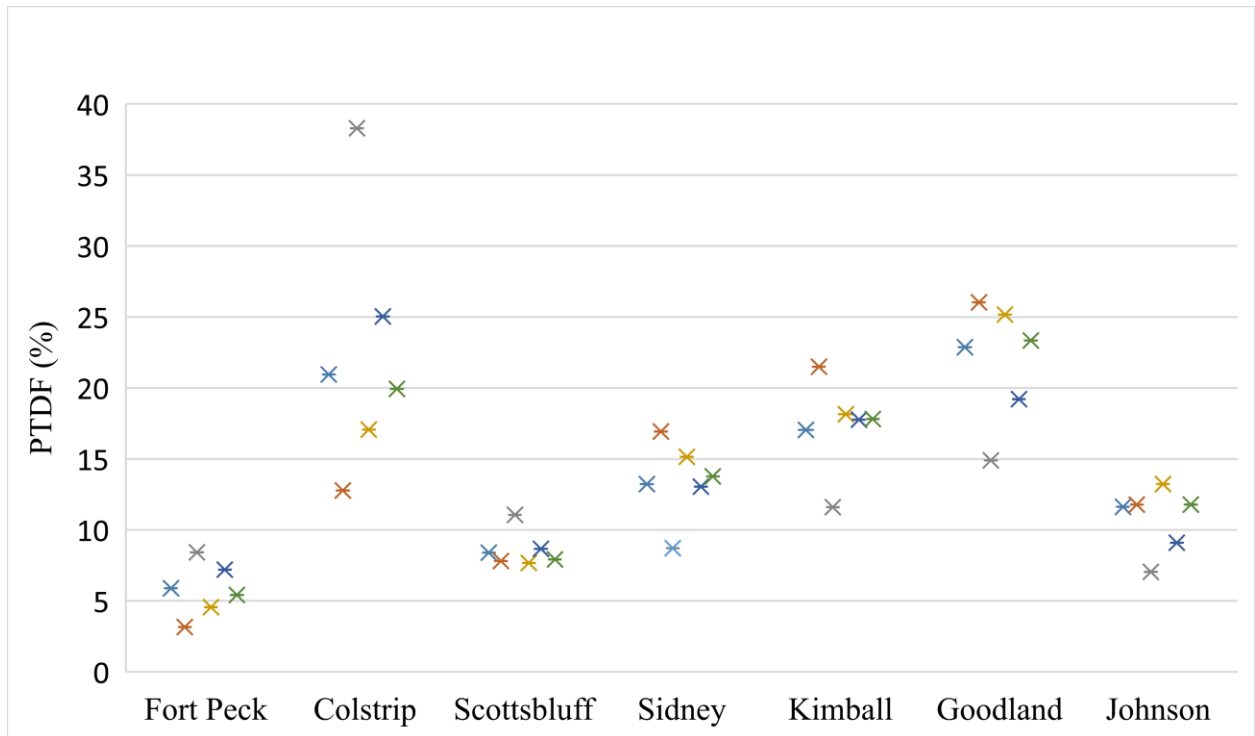


Figure 2.7 PTDFs of AC Ties for Different Transfer Scenarios

Such analysis is helpful in showing the expected range of the distribution of flows across the Interface, which can potentially indicate locations where transmission system upgrades may be needed or prioritized.

2.4.2 Available Transfer Capability Analysis

ATC analysis determines the maximum incremental MW transfer possible between two parts of a system without violating any specified limits. The transfer limits were calculated in each direction i.e. West to East, and East to West. PowerWorld Simulator has three methods for solving ATCs,

with the Single Linear Step approach being the most common. This method of ATC analysis uses sensitivities about the present system state. These sensitivities are embodied in the PTDF and Line Outage Distribution Factor (LODF) calculations.

For example, for a transmission line with a limit of 10 MW, present loading of 5 MW and a PTDF of 10%. The estimated maximum transfer without overloading the line is,
Transfer Limitation = (Limit – Present Loading) / PTDF = (10 – 5) / 0.1 = 50 MW

When including contingency analysis, the OTDF (Outage Transfer Distribution Factor) and linearized estimates of post-contingency flows are used to determine the Transfer Limitation.
Transfer Limitation = (Limit – Post-Contingency Loading) / OTDF

For the base case (i.e. with no contingencies), the first limiting element of the Interface is encountered at a transfer value of 4800 MW for the East to West direction, and at 6600 MW in the West to East direction. This happens to be the Hardin-Colstrip tie of the Interface, which corroborates the PTDF results. When non-Interface limiting elements are considered, these values are lower with 1800 MW for East to West and 2000 MW for West to East transfers, with the same few limiting elements resulting for multiple transfer scenarios. This is indicative of the potential for major improvements in transfer capacity with a few modest changes or rating upgrades.

When N-1 contingencies are applied, the first limiting element of the Interface is Lamar-Johnson at a 5000 MW West-East transfer across the Interface. For East-West transfers, the transfer limit is around 3500 MW with Hardin-Colstrip and Lamar-Johnson reaching their limits.

Note that these results are for a dc analysis, which ignores reactive power. The next subsection briefly discusses transfers with the full ac power flow considered.

2.4.3 MW Transfers with AC Power Flow

So far, dc power flow or linearized methods were used to estimate maximum possible transfers. Here we use a full ac power flow solution with different transfers across the interface and identify each transfer limit (i.e. transfer value until which a power flow solution is obtained). For simplicity, areas are chosen arbitrarily in the East and West to set up MW transactions. The transfer limit in this case is around 2300 MW East to West (OK to CO transfer) and 2500 MW West to East (WY to NE transfer). These values correspond well with the transfer capacity estimated for the real EI-WI interconnection studied in this project.

3. Dynamics

3.1 Introduction

The main part of the project has been setting up and performing the dynamic simulations. Electric grid time-domain simulations can be divided based upon the time scale of the underlying dynamics, with [17] presenting four groups starting with wave phenomena (with a time scale of less than a microsecond) and going out to thermodynamics (ranging up to many hours). The time-domain simulations considered here will be in the middle of this range, a scale in which the electric grid is modeled using a phasor representation. As noted [18] and [17], this considers aspects of rotor angle stability, voltage stability, frequency stability, and to some extent converter-driven stability. The integration step size used was $\frac{1}{2}$ electrical cycle (8.333 ms), through the use of multirate methods [19], [20] allows for accurate modeling of the much faster models associated with devices such as exciters, loads and some renewable generators.

While historically such studies were known as transient stability simulations [21], here we will use the generic term “dynamic simulations”. As is common, the simulations are initialized from a power flow solution, and then a contingency scenario is applied to the grid and the goal is to determine the time-domain response. The simulations considered here are assumed to have a fixed duration ranging from seconds to four or six minutes.

This section present results from the actual EI and WI system in overview form, and more detailed results for the synthetic grid. One of the challenges of this project had been dealing with the sheer magnitude of the size and complexity of the grids, and the amount of data that could be produced during a dynamic simulation. For the actual system, the model contained about 110,000 buses, 13,700 generators, 246 different types of dynamics models, more than 61,000 dynamic model instances, and more than 200,000 differential equations. One of the reasons for the larger number of dynamic model types was due to the original dynamics data coming from the WECC sometimes using slightly different models than those used in the EI (e.g., two different types of EXST1 exciters needed to be modeled). The situation was somewhat simplified for the synthetic grid, which has 80,000 buses, 25 different types of dynamics models, 60,000 dynamic model instances and 237,000 differential equations. Determining how to best present this information to the user has been a part of this project and is presented partially in Chapter 4 and more completely in two recently submitted publications [22], [23].

3.2 Actual Electric Grid Results Summary

For this project, a wide variety of different dynamic simulations have been run on both the heavy and light load scenarios. The key limiting characteristic on interconnecting the EI and WI is during generator loss contingencies in the WI, approximately 75 to 80% of the lost power will flow through the Interface from east to west since the governor response takes place uniformly through the interconnect and most of the generation is east of the Interface. During generator contingencies in the east approximately, 20 to 25% of the lost power does flow through the Interface from west to east, but since the percentage is substantially smaller, this is viewed as a much less severe constraint. As an example, Figure 3.1 shows the dynamic variation in the Interface MW flow for the loss of 2700 MW of generation in the WI with positive flow in the figure from east to west. As can be seen in the figure, the power across the Interface changes from a pre-contingent value of 150 MW to around 2600 MW, and seems to settle around 2200 MW. That is, a total of nearly 2100

MW flows on the Interface from east to west to make up for the 2700 MW outage in the WI. Thus the interface flow is about 80% of the generation lost. This governor response flow issue is fundamental to interconnecting large grids and does require any interface joining two such larger grids be able to handle this flow (at least until AGC can respond). In particular for the EI and WECC, there needs to be sufficient tieline capacity to handle the required most severe single contingency (MSSC).

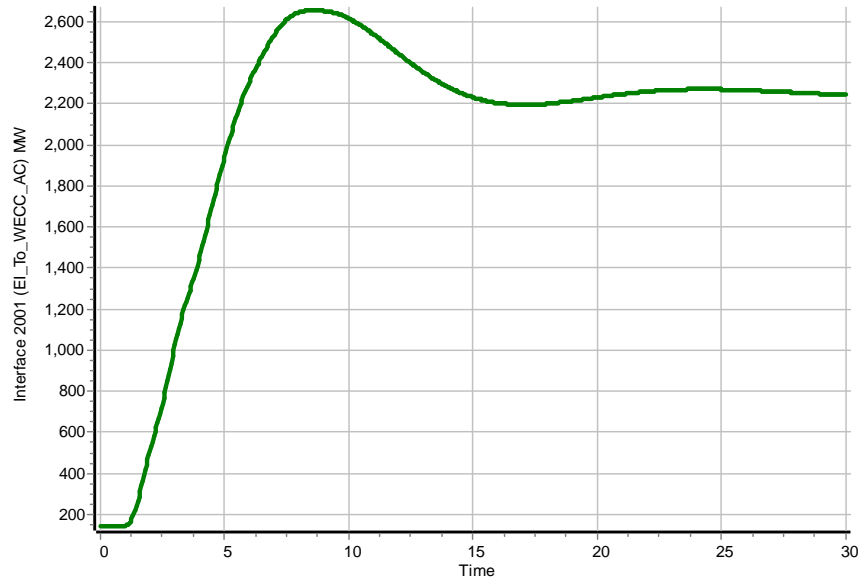


Figure 3.1 MW Flows on the EI-WI Interface

One key difference in the WECC frequency response for WECC generator loss contingencies is there is substantially less frequency drop, at least after the first two seconds. As an example, Figure 3.2 compares the frequency variation at three WECC buses for a generator loss contingency with the thin lines showing the response with the WECC operating as it is today (i.e., separated) and the thick lines showing the response with the combined system. The reason for this is, of course, because as shown in Figure 3.1, lots of makeup power will quickly flow from the EI across the Interface into the WECC. From an EI perspective, there was very little additional frequency impact either from WECC contingencies or EI contingencies. Figure 3.3 shows the frequency variation for the 43,400 substations with the left figure showing the frequencies in the EI and the right one those in the WECC.

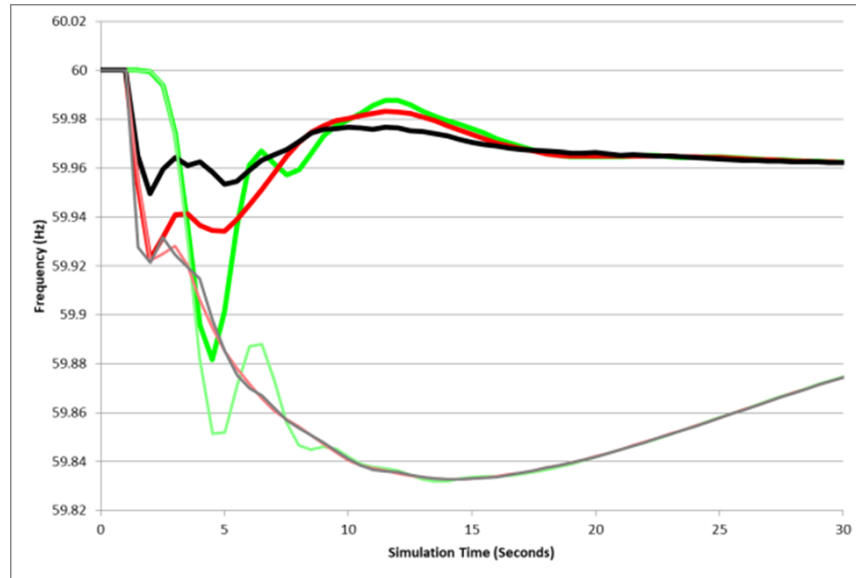


Figure 3.2 WECC Bus Frequencies as Thin (Thick) Lines for Separate (Combined) Systems

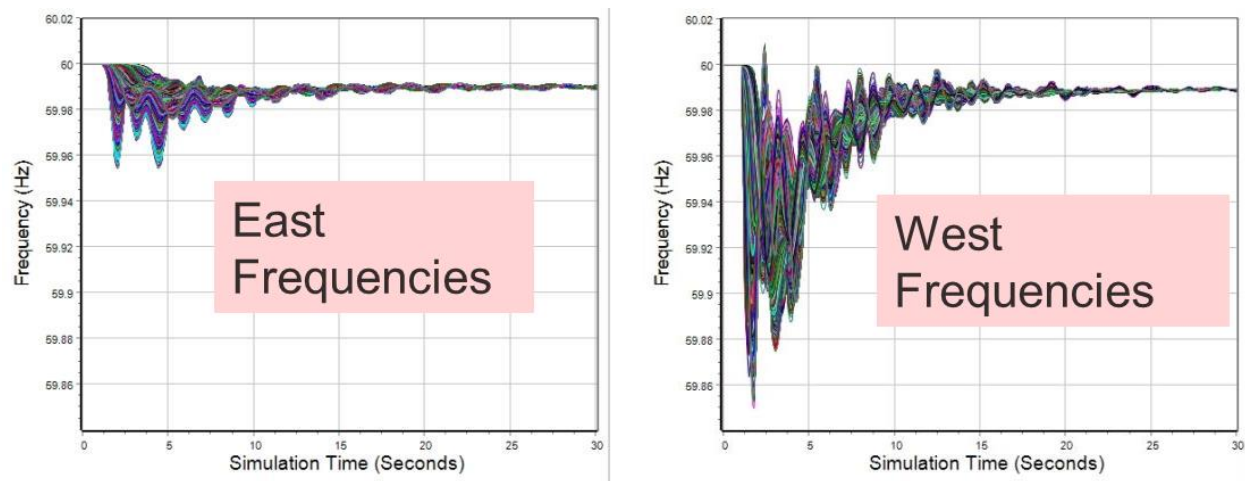


Figure 3.3 Frequency Variation at All Substations for a WECC Generator Loss Contingency

3.3 Long-term AGC Modeling

As has been noted, following any disturbance about 75% to 80% of the governor response will occur in the EI, with the flow increasing from east to west across the Interface if the contingency is generation loss in the WECC and the opposite direction for generation loss in the EI. By themselves, the governors do not restore the system frequency to its setpoint value; rather this is done by the automatic generation control (AGC) utilizing the balancing authority area control error (ACE) signal. The ACE has a frequency component,

$$ACE = P_{actual} - P_{sched} - 10\beta(freq_{act} - freq_{sched}) \quad (3.1)$$

where β is the frequency bias; it has a negative sign, units of MW/0.1 Hz and is about 1% of the peak load/ generation.

This AGC response usually takes place on the order of minutes, so it has not traditionally been included in standard transient stability level dynamic simulations. However, for this project we did want to get a feel for how the combined system would perform for longer-term simulations. Since the used simulation software does provide some support for AGC modeling, this response was included in some of our studies. This was setup by defining all areas as being on AGC control, assigning to each a β value, a frequency measurement bus, an ACE MW deadband and a set of scheduled transactions. For each area, the unspecified transactions were modified so the starting ACE for each area is zero. In addition, each generator also needs an AGC controller. The AGC controller has a MW minimum and maximum value, and a participation factor. Given that this information is not available, defaults were used in the initial studies (min/max values from the power flow, and its participation factor proportional to its maximum MW value). Then during the simulation, the area ACE is calculated, with the ACE error sent to the generator AGC controllers, with the desired MW control change proportional to its participation factor. This error is then used to change the governor setpoint values.

For the simulation presented here, the contingency is again a loss of generation in the WECC. Initially, as before, the change in the generation is handled by the governor response. But then in these extended simulations bilateral transactions are implemented between the area that lost the generation and other nearby areas, with the transactions ramping up over a specified time period. For the initial AGC simulations, which ran for four minutes with the transactions starting at 30 seconds and ramping over two minutes, using the standard integration step size of $\frac{1}{2}$ electrical cycle, a 0.08 Hz oscillation was observed. This was concerning since low frequency oscillations with a similar frequency had been reported with large-scale interconnection studies in Europe [5]. An example of the impact of this oscillation on the Interface flow is shown in Figure 3.4. However, using the modal analysis techniques from [24] and [25], the source of this oscillation was quickly determined to be from a single large unit more than a 1000 miles from the interface with what appears to be incorrectly tuned governor PID values. The oscillation was removed when this single generator was taken off of AGC control, with the results shown in Figure 3.5 (with the transactions now starting at one minute and ramping over four minutes). The conclusion, at least for this scenario, is the interconnected grids are stable even when AGC response is considered.

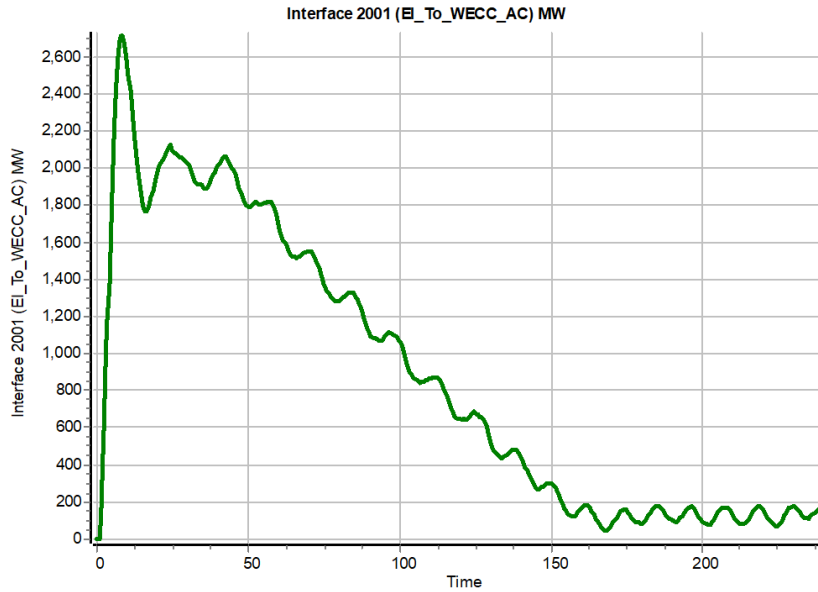


Figure 3.4 Initial AGC Response Simulation with a 0.08 Hz Oscillation

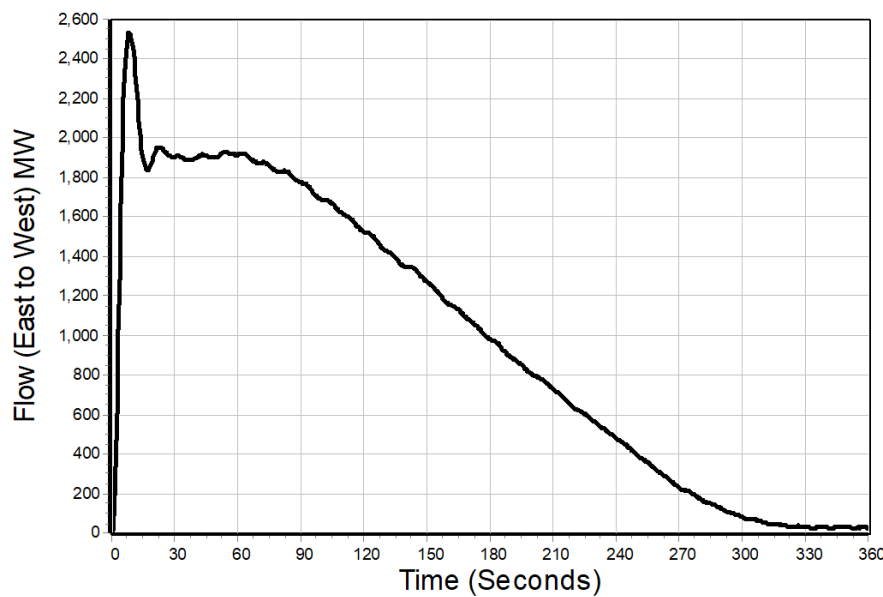


Figure 3.5 Modified System AGC Response

3.4 Synthetic Grid Simulation Results

As noted at the beginning of this chapter, for this project a synthetic 80,000 bus synthetic grid was setup and preliminary studies performed to illustrate issues associated with the interconnection of large-scale grids with an eye towards providing a test system for other researchers. The oneline for the system is shown in Figure 2.6, but much more importantly, the full system model is available at [16]. Of course with access to the model itself researchers are free to explore any number of contingencies or modifications to the number of tielines, with a rather severe contingency of the

outage of 4200 MW of generation (located at buses 2040843, 2040844 and 2040845) used for illustration here. As was the case in the previous section AGC response is also modeled with bilateral area transaction ramping. For simulation and display convenience these transactions were setup to start faster than would actually occur (here at a simulation time of 30 seconds) and ramp faster (here with ramping between 30 and 90 seconds). The total simulation ran for 120 seconds.

There is a wide variety of different ways to present results with this section giving some illustrations with additional results available in [23]. The first three figures (from Figure 3.6 to Figure 3.8) show the Interface MW flow (of course now for the synthetic grid) and the voltage frequency and magnitude response at ten selected buses (picked from throughout the West) for the first 30 seconds of the simulation. The next four figures (from Figure 3.9 to Figure 3.12) show the response of the Interface MW and the selected buses over the whole two-minute simulation. Just based on this small sampling of results the simulation appears to be stable.

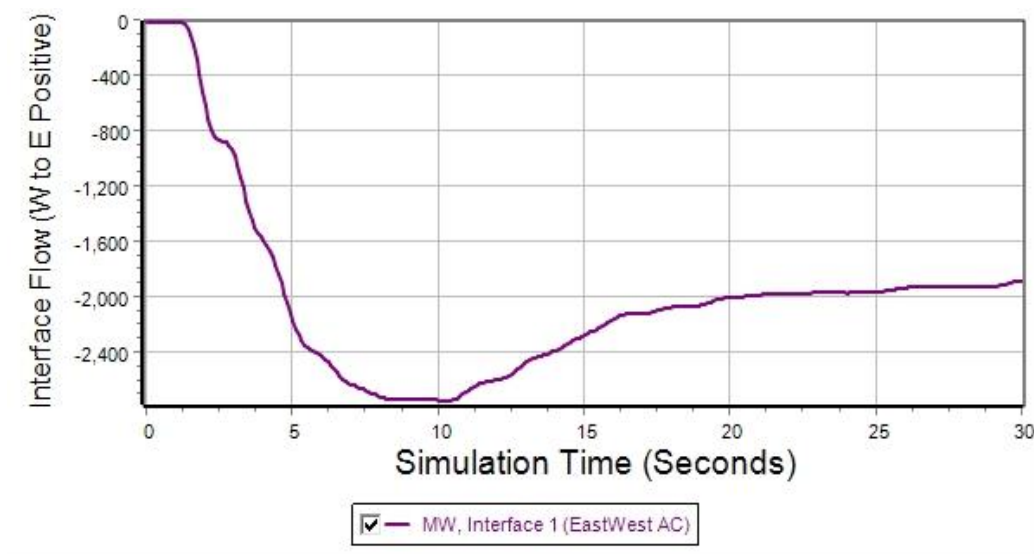


Figure 3.6 Interface Flow MW (West to East Positive) Over 30 Seconds

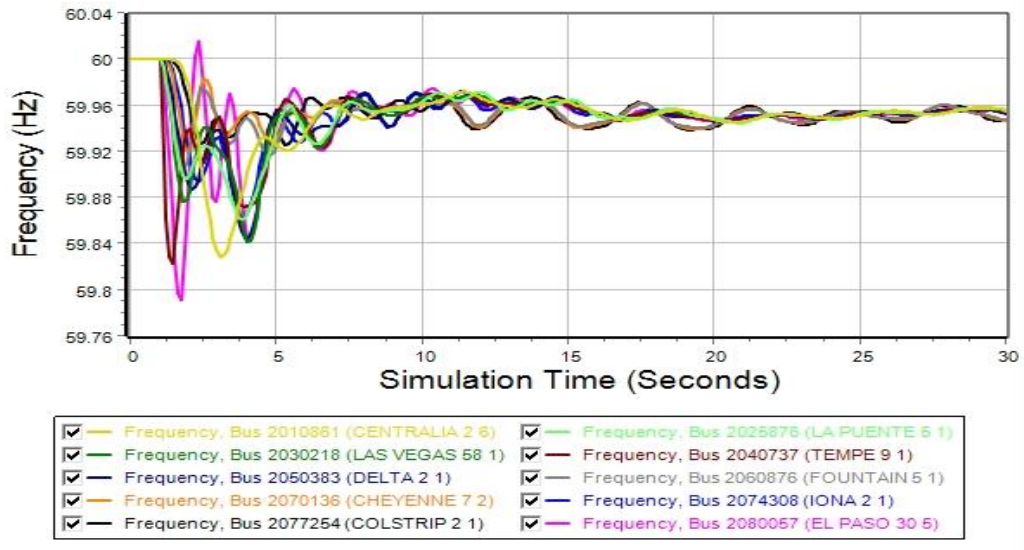


Figure 3.7 Frequency Response at Ten Buses in the West Over 30 Seconds

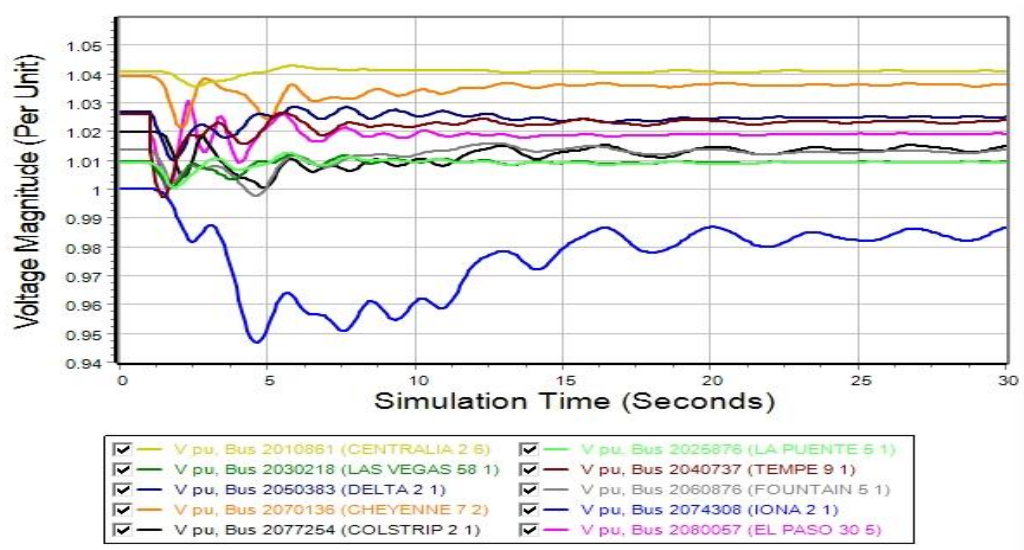


Figure 3.8 Voltage Magnitude Response at Ten Buses in the West Over 30 Seconds

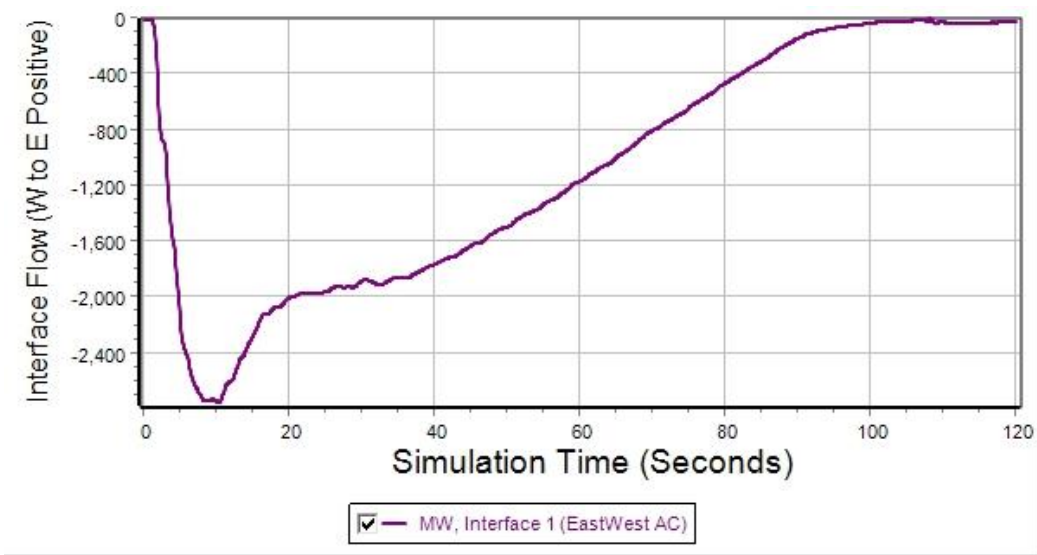


Figure 3.9 Interface Flow MW (West to East Positive) Over 120 Seconds

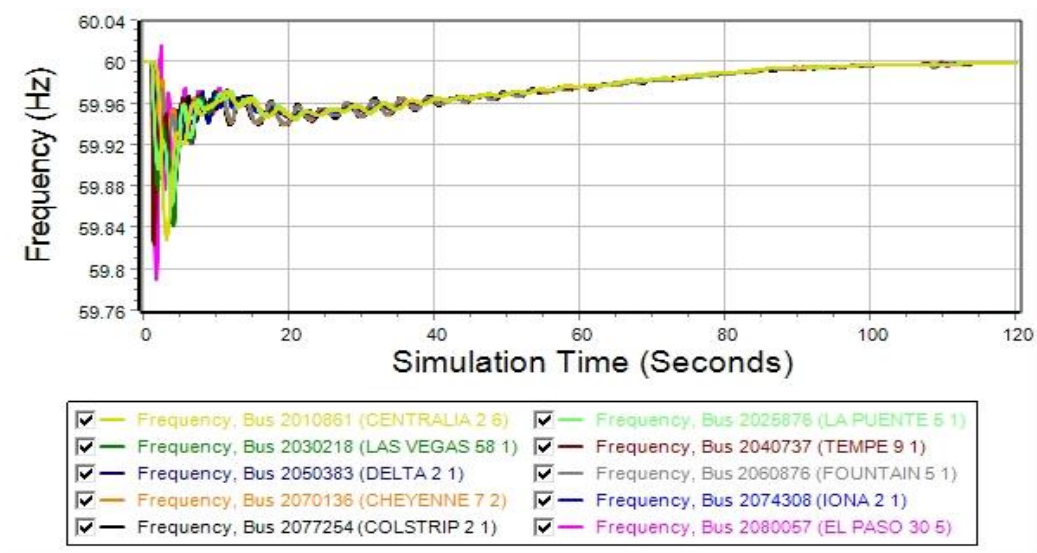


Figure 3.10 Frequency Response at Ten Buses in the West Over 120 Seconds

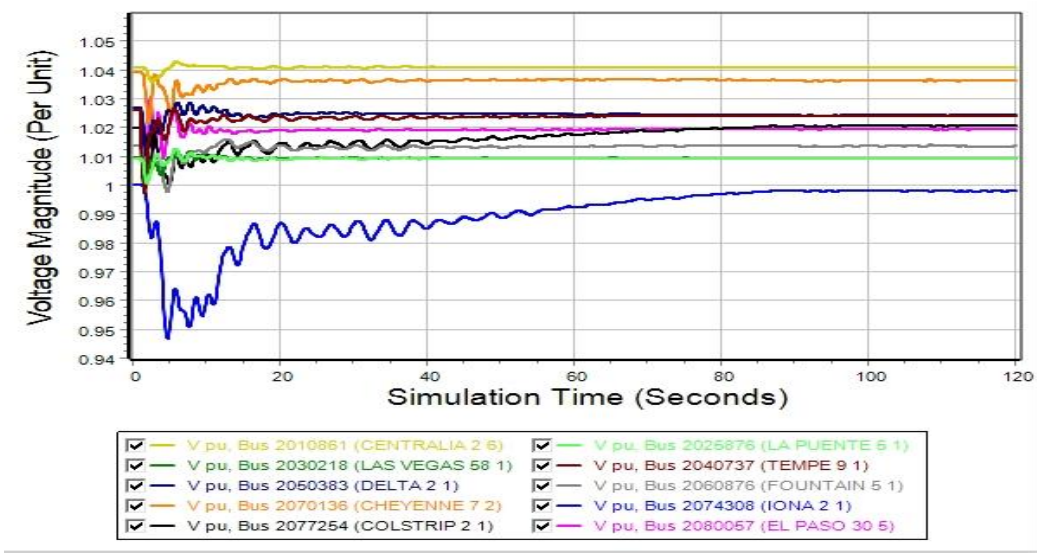


Figure 3.11 Voltage Magnitude Response at Ten Buses in the West Over 120 Seconds

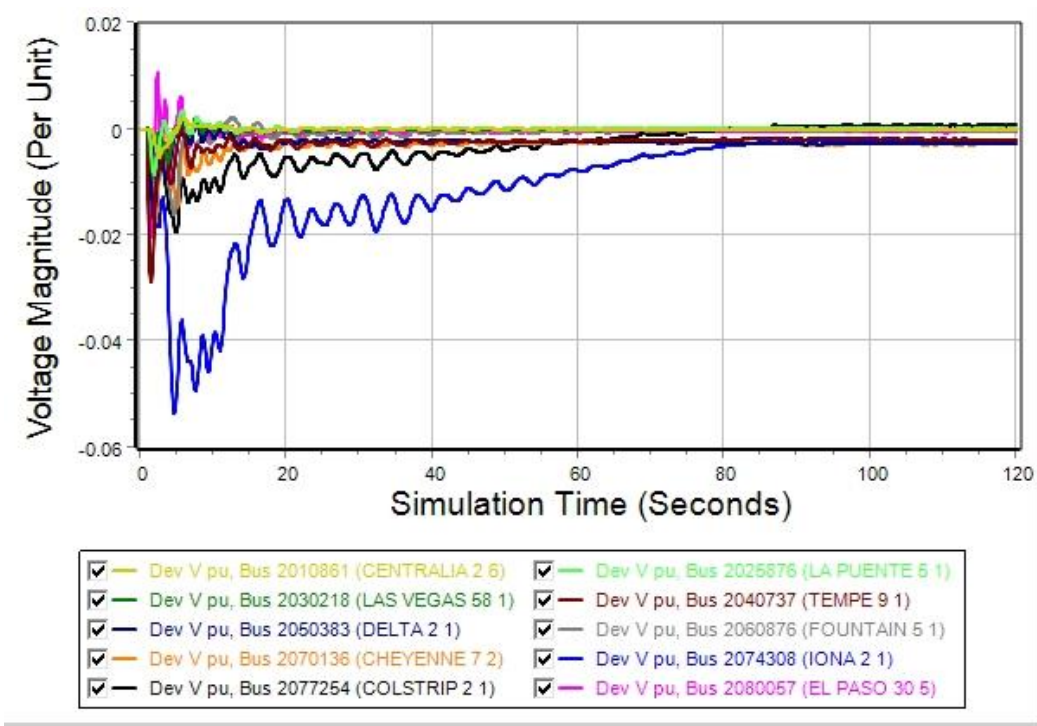


Figure 3.12 Voltage Magnitude Deviation at Ten Buses in the West Over 120 Seconds

Plotting the response of only a few variables provides limited understanding of the overall system response. In order to understand the full system response these graphs need to be supplemented with other techniques. One approach would be to plot all of the signals of a particular type. Graphing all of the 80,000 bus frequencies in Figure 3.13 and all of the voltage magnitudes in

Figure 3.14 provides a better understanding of the overall system response to the event. While the individual signals cannot be determined from such figures, they do provide the overall envelop of the response. This example demonstrates that all frequencies settle back to 60 Hz with the AGC response, the voltage magnitudes settle back close to their original values for the generator contingency, and there is a part of the system in which the voltage recovers slowly.

An approach to visualize the spatial variation in system quantities such as voltage magnitude deviation at a particular time would be to use a contour [34]. This is illustrated in Figure 3.15 in which a red/blue contour is used to show the voltage magnitude variation at ten seconds. The contour can be combined with other objects such as GDVs. Here the GDV summary objects (described in more detail in Chapter 4) are super-imposed on the contour with the yellow/magenta rectangles showing the change in MW generation in different parts of the system in response to the contingency and the black GDV summary flow arrows showing the change in MW flow on the transmission grid.

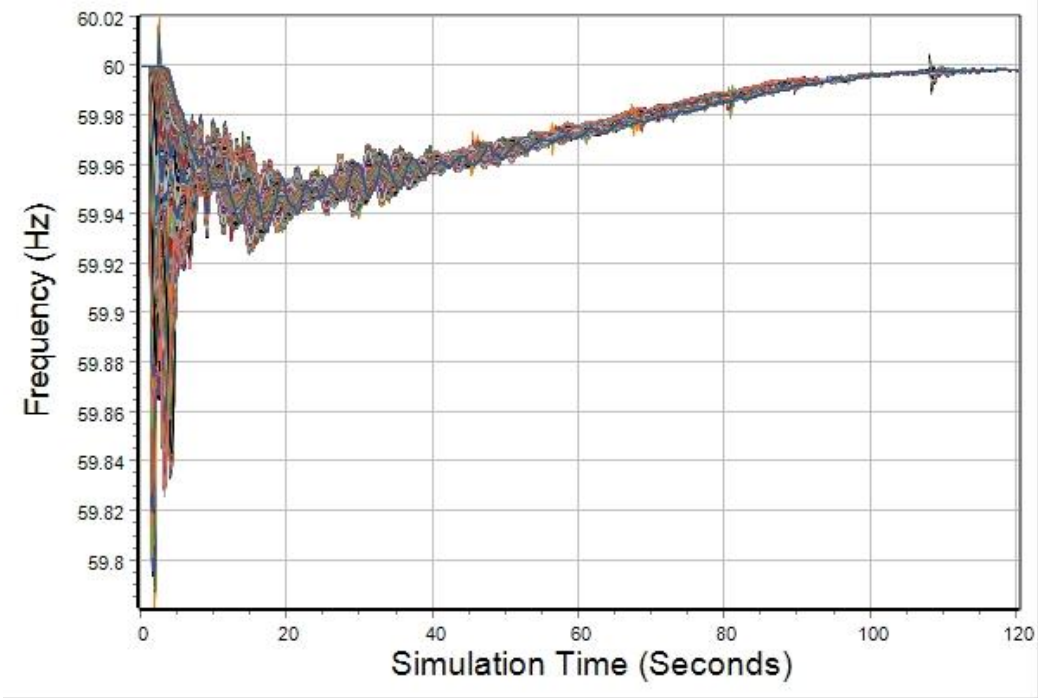


Figure 3.13 Frequency Response at All 80,000 Buses

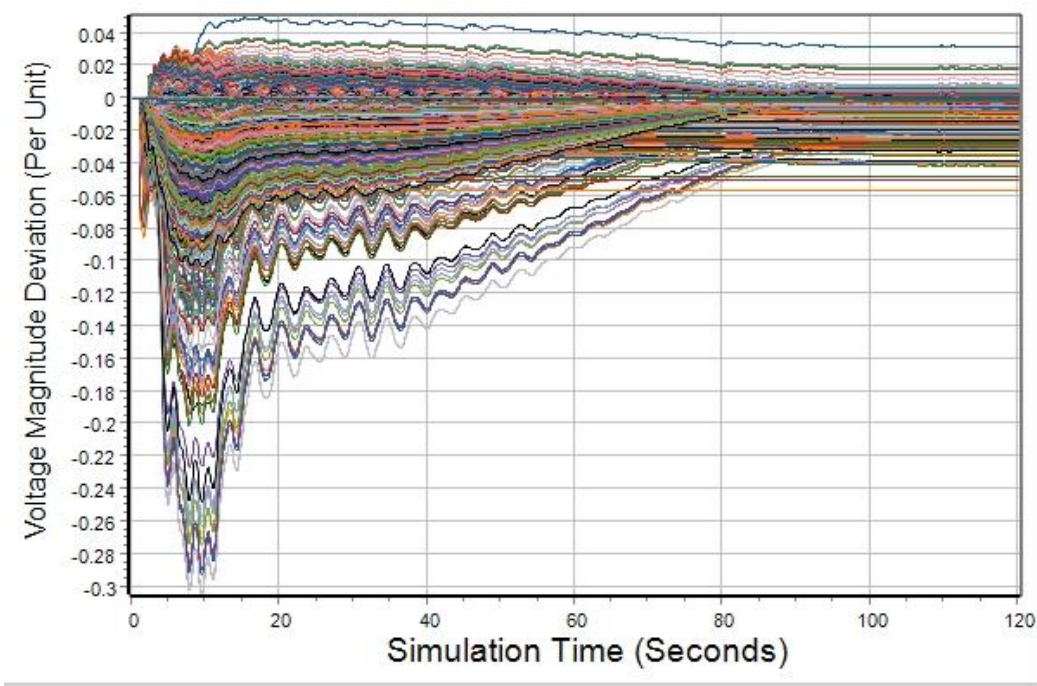


Figure 3.14 Voltage Magnitude Deviation at All 80,000 Buses

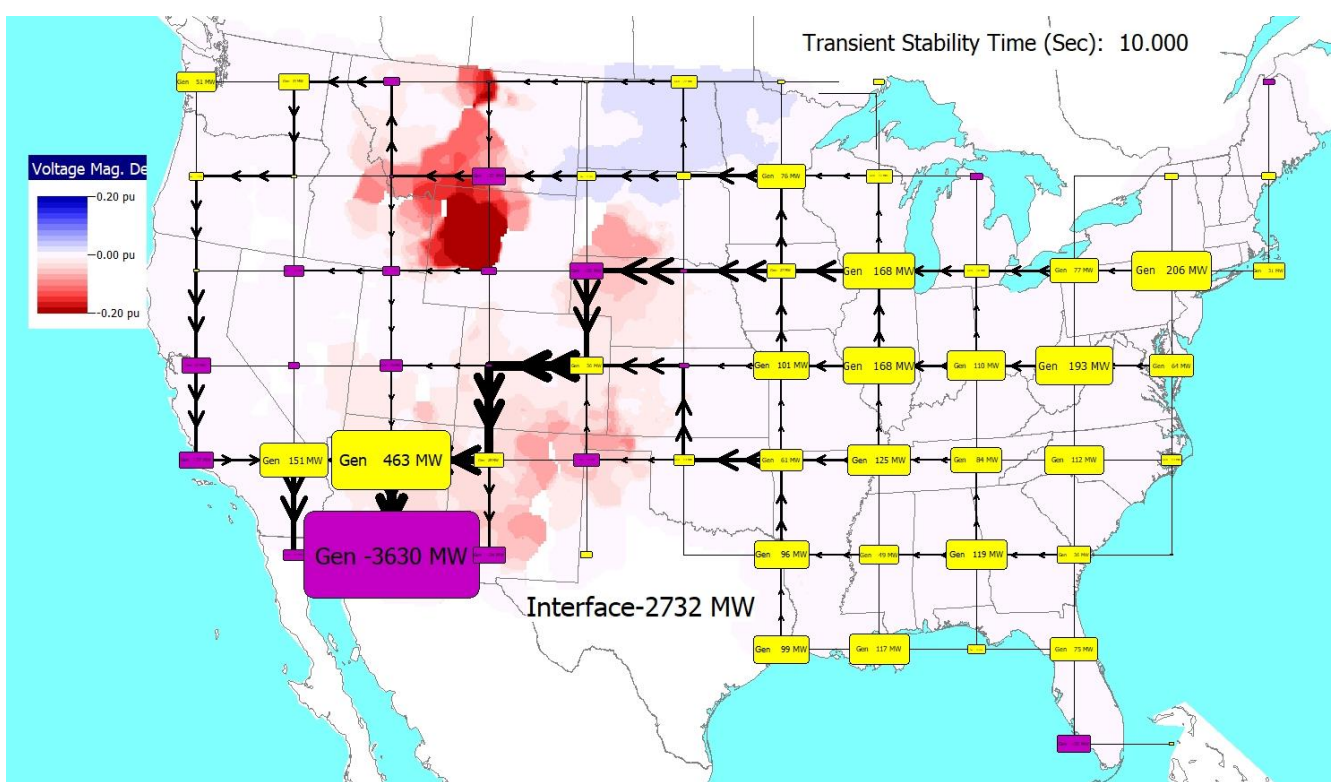


Figure 3.15 Visualization of System at Ten Seconds Using Voltage Contour and GDV Summary Objects

4. Geographic Data Views for Wide-Area Visualization

4.1 Introduction

A major challenge associated with this project has been understanding what is occurring in the large scale electric grids, particularly when they could be subject to unusual operating conditions such as those associated with a new ac interconnection. This chapter is a summary of the use of geographic data views (GDVs) submitted for publication in [22]. In short, GDVs are electric grid display objects whose location is dynamically determined from geographic information embedded in an electric grid model. The 82,000 bus synthetic electric grid (now including Texas) is used here to show how GDVs can help provide wide area understanding of values such as generator outputs, switched shunt values, voltages, and transmission line flows.

The term situational awareness (also called situation awareness) (SA) was popularized in the electric grid literature as a result of its prominence in the North American August 14, 2003 Blackout final report [26]. As defined in [27] and discussed in [28], SA is intuitively “knowing what’s going on” and, more formally, as “the perception of the elements in the environment within a volume of time and space, the comprehension of their meaning and the projection of their status in the near future.” In the blackout report, lack of SA was one of the four causes of the event. The term is now widely used in electric grid operations and has been the subject of a variety of papers including [29], [30], and [31].

Associated with wide-area electric grids, the concept of “knowing what’s going on” doesn’t just apply to operations, but rather the large number of engineering studies that are used to ultimately support the actual operations. These include many different studies and simulations done by many different groups including the real-time support engineers, power marketers and traders, long-term planners, and ultimately the researchers developing new algorithms and techniques. The concept of SA was originally introduced for dynamic systems, it has long been used in static situations as well, including the military [32]. The focus here is on techniques applied to larger scale systems to help people maintain SA during electric grid engineering studies such as power flow, contingency analysis, and time-domain simulations.

The power flow is certainly one of the most widely used electric grid analysis tools, and maintaining SA during a power flow study is straightforward if the system is small. However, with electric grid models often having tens of thousands of buses, as is the case here, it can sometimes become difficult to fully comprehend study results. This is not just due to the model size but also its complexity. The quantities of interest can get quite long, including the bus voltage magnitudes and angles, line flows, generator real and reactive power outputs, changes in automatic controls such as switched shunts and transformer LTC or phase positions, and sometimes other values such as those associated with geomagnetic disturbance studies (GMDs) [33]. The variables of interest expand further when the results include sensitivities or the study includes contingency analysis, OPF, security-constrained OPF, or time-domain simulations.

Over the years, several different information management and visualization techniques have been developed to help engineers maintain SA during such studies. These include onelines, tabular displays, intelligent alarming, 3D displays and color contouring [34], [35], [36], [37] and [38].

This chapter presents new developments in the use of geographic data views (GDVs) for wide-area electric grid visualizations.

4.2 Geographic Data Views

The purpose of GDVs, which were first presented in [39] and [40], is to provide a fast and flexible way to show large amounts of geographically-based information for larger-scale electric grids. GDVs use geographic information embedded in an electric grid model to draw symbols on a display with the symbol's appearance dynamically determined by the electric grid model object values. Hence, a key requirement for the GDV approach is that at least some of the electric grid components have geographic coordinates such as the latitude and longitude of the substations.

Geographically based information exists for real electric grids though historically it was often not included in the transmission system models used for power flow analysis. This is now rapidly changing, partially because this information is now required (at least in North America) for GMD risk analysis studies, and partially because of the now widespread availability of the grid information in geographic information systems. Geographically-based large scale synthetic electric grids are also now available with substation latitudes and longitudes [41], [42] containing dynamic model parameters needed for time domain simulations [15].

Often, wide-area transmission grid visualization is done using either a fully geographic approach (e.g., as done with Google Maps) or in a pseudo-geographic approach in which the geographic locations are only approximate (such as in an electric utility control room map board display). The advantage of the fully geographic approach is it allows easily coupling with other geographic information, such as weather. A disadvantage is that the grid equipment itself has a very small geographic footprint and often can be densely packed in areas such as urban centers. The pseudo-geographic approach sacrifices some geographic exactness for display clarity.

This chapter demonstrates the use of GDVs using the 82,000 (82K) bus synthetic grid covering the Conterminous (Contiguous) U.S. The 82K grid has the buses mapped into 41,012 electric substations, with geographic coordinates provided for each substation; it has 104,125 transmission lines and transformers (branches). In addition, the grid is divided into areas, with 76 areas for the 82K bus model.

The oneline for this grid is in Figure 4.1 with the line color on the display used to show the transmission line's nominal voltage (blue for HVDC, green for 765 kV, orange 500 kV, red 345 kV, purple 230 kV, and black for lower voltages). The green flow arrows superimposed on the branches to show the direction and magnitude of the real power flow. While such onelines can certainly be helpful for electric grid study SA (with example useful techniques given in [43]), SA can be enhanced through the use of GDVs.

The GDVs symbol's initial display location is usually determined by geographic information from the object associated with the GDV. For some objects, this information is directly available, such as the location of a generator or substation. For others, such as an electrical area that is defined as a set of buses, its location needs to be derived (e.g., an area's location is the average of the location of its component buses). These initial locations might then be modified for display clarity.

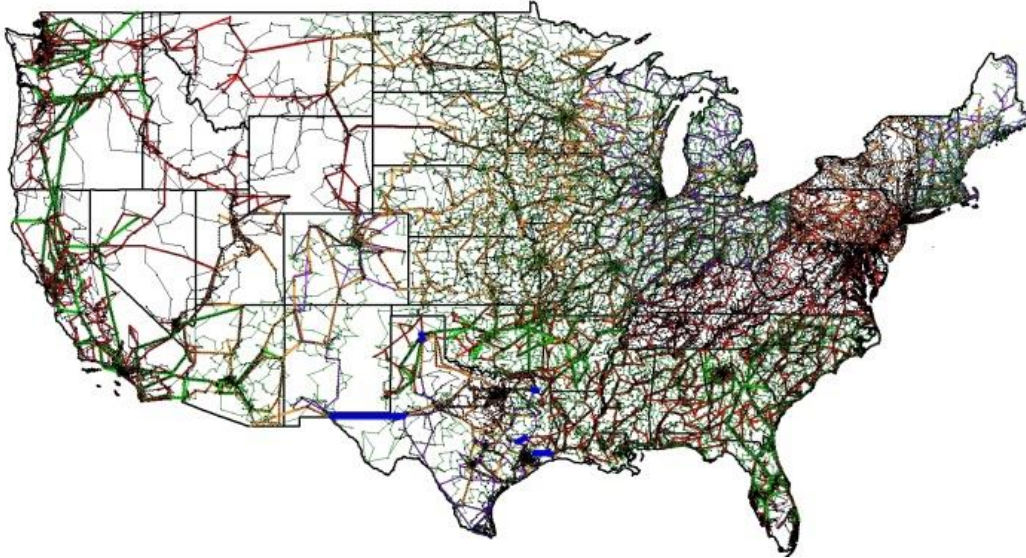


Figure 4.1 82,000 Bus System Online

The GDV symbol display attributes are then dependent upon one or more field values from the linked electric grid object. Common display attributes include the symbol's size, fill color, border thickness, and border colors. The field values can be almost anything, with real power output being one example. Figure 4.2 shows an example of the use of GDVs to show the 76 areas from the 82K grid, with the size of each proportional to the area's total generation, and the color dependent upon whether the area is exporting (red) or importing (blue) power.



Figure 4.2 82,000 Bus System Area GDVs

During a power flow solution people usually know the changes that they explicitly made. The SA challenge is to understand the response of the sometime quite involved automatic controls,

including the changes in the generator real and reactive power outputs, the switched shunts, or area interchange (Figure 4.2). Other values that could be shown using GDVs include the LTC transformer tap changes or phase angle regulator changes. However, this is not to imply that all important values are best illustrated using GDVs. As noted earlier, regular onelines and tabular displays are important and often best for showing essential system-wide SA values such as total island load, generation and its slack bus output. Another important SA quantity, the per unit voltage magnitudes, could be shown using color contours [34].

While the concept of GDVs is general, before moving on it will be useful to present several particulars to our implementation and associated user interface (UI) that can be helpful from an SA perspective. First, all of the GDVs are linked to their associated electric grid objects with the UI making it easy to get additional information about the object such as its dialog. Second, all of the GDVs are grouped into styles with the UI also making it easy to view the GDV's style dialog. The style defines all of the GDV attributes, such as what object values (e.g., MW) to map to what display attributes (e.g., display size or color). While a linear mapping is common, the actual implementation supports piece-wise linear mappings. The ability to quickly access the style provides several advantages such as a user being able to see the mapping used and, if desired, change it. Multiple styles can be used on a single display, though for clarity all the examples here only use a single style. Third, in the UI the GDVs can have up to three display lines, making it easy to show its ID and sometimes numeric field values.

Fourth, the UI makes it quite easy to create the GDV displays. For example, using predefined backgrounds the figures shown here can each be created in just a few minutes. Fifth, while the GDVs are automatically placed on the displays using embedded geographic information, they can be manually repositioned such as to avoid overlaps. Sixth, while simple to create, the GDV displays can be stored to allow them to be used repeatedly. Seventh, in the approach implemented here the GDVs can be used to show either actual power system values, or differences between two solutions. Example usages include comparing the changes due to a power flow or OPF solution, or showing how quantities varied during a time-domain simulation. Last, the UI used here has been developed to allow GDV use with a large variety of different object types. For example, in a recent large system study we needed to gain better SA associated with a large number of contingencies and associated remedial action schemes (RASs) [44]. Since both could be placed geographically (by averaging the coordinates of their component objects) we were able to use GDVs quite effectively.

However, GDVs do have a potential shortcoming related to their use of display space. As is readily apparent, overlap can be a problem. For some object types, such as generators, multiple objects may be at the same geographic location. Even when the locations are different because of how the grid is structured often with a large number of devices in small geographic regions (e.g., urban areas) significant overlap can occur. There is an inherent tradeoff between the GDV's display size and this degree of overlaps. The next two sections provide some techniques for dealing with this issue.

4.3 Use of Layout Algorithms

GDV display placement involves a tradeoff between display clarity and geographic accuracy. As noted in the beginning of the previous section, the use of a pseudo-graphic approach, in which the display space itself is not strictly geographic, is one solution. The alternative is to keep the display itself geographic, but to be more approximate in the GDVs actual placement. Two such approaches are presented in [45] and [46]. With the Pseudo Geographic Mosaic Displays (PGMD) the display design goal changes from geographic accuracy to full utilization of the display (screen) space but with only an approximate geographic precision. As with the other GDV displays, all the GDVs are linked to their associated objects making it easy to get more detailed information and/or do control.

An alternative is to utilize a force-directed graph drawing algorithm to move the objects apart, sacrificing some geographic accuracy for improved display clarity. Force-directed algorithms are common in many domains, with the concept initially presented in [47] and some recent electric grid applications in [48], [49], and [50]. The idea is to better layout the display objects by assuming each is subject to repulsive forces, pushing it away from its neighbors and attractive forces pushing it towards other objects or a fixed point. Then an iteration is run until an equilibrium is achieved.

Over the years, a number of different repulsive and attractive force functions have been proposed, with a Coulomb repulsive function common in which the force decreases with the square of the distance, and a Hooke attractive function that mimics the linear force of an ideal spring. These functions are used here, with the Coulomb “charge” of each GDV proportional to its area, resulting in the larger GDVs getting more display space. Given that each GDV has a geographic location, similar to [50] the attractive force is anchored there. In addition, a static friction force is applied if the GDV is at this location, causing a tendency for it to stay put. For objects at the same location, separate initial perturbations are applied to separate them. Normalized scaling values are also provided on each force to allow the display’s appearance to be easily customized.

Key to implementing this algorithm on larger displays is to reduce the otherwise $O(n^2)$ computation associated with computing the repulsive forces. By taking advantage of the typical electric grid structure of GDVs distributed fairly uniformly across the display and that the Coulomb force decreases with the square of the distance the computation can be reduced substantially by just including in the calculation those GDVs within a given radius. Various heuristics can be used to determine this radius, but a value that gave reasonable results was four to six times the width of the largest GDV. The set of neighbors within this distance for each GDV can be determined with $O(n \log n)$ computation by setting up a k-d tree data structure. Optionally, the number of total neighbors could also be limited recognizing that the GDV densities could vary across a grid.

To demonstrate that this algorithm works on large systems, Figure 4.3 shows an initial display from the 82K grid with 4055 GDVs for substations with non-zero generation. The color of each GDV is shaded based on its percentage reactive power output. Figure 4.4 shows the display after application of the force-directed layout algorithm with boundary enforcement. Overall, the algorithm took about 12 seconds with an average of 119 neighbors per GDV considered for the Coulomb forces. While admittedly the individual substations are difficult to see in these small figures, on a computer screen with support for zooming and panning it is relatively easy to use the display to get a good feel for what is going on with respect to the overall generator reactive power

outputs. Both figures use a selective color mapping in which only reactive power loadings above 80% of the maximum limit are shaded red and those below 80% of the minimum limit are shaded blue. This can enhance SA by making these outliers stand out by taking advantage of pre-attentive processing [51]. One takeaway from Figure 4.4 is that the associated power flow has an unrealistic number of generators operating with low power factors.

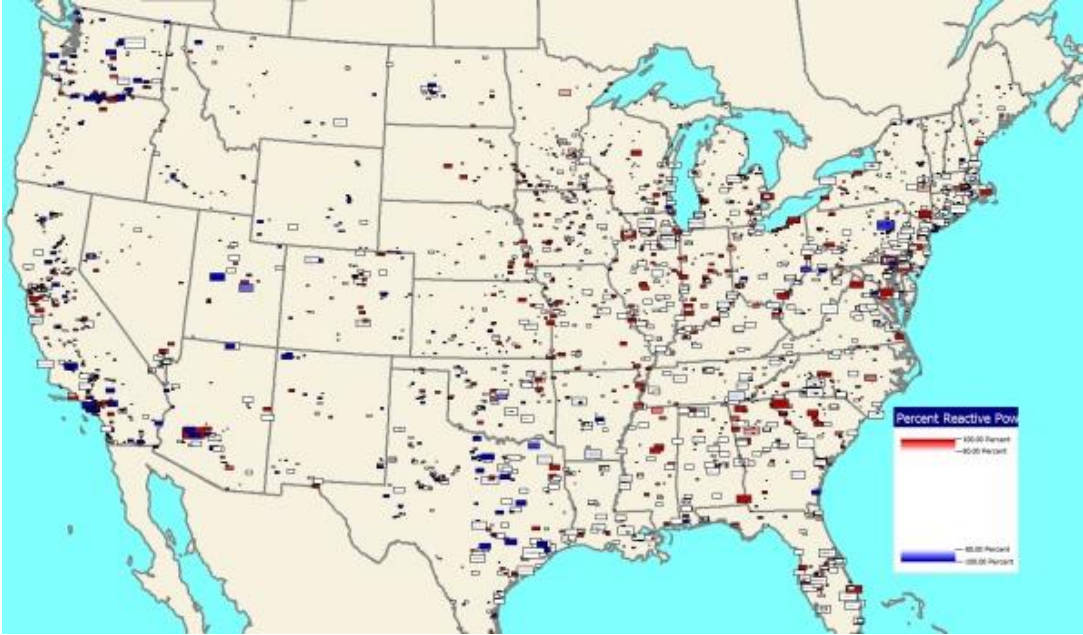


Figure 4.3 82,000 Bus Grid Substation GDVs

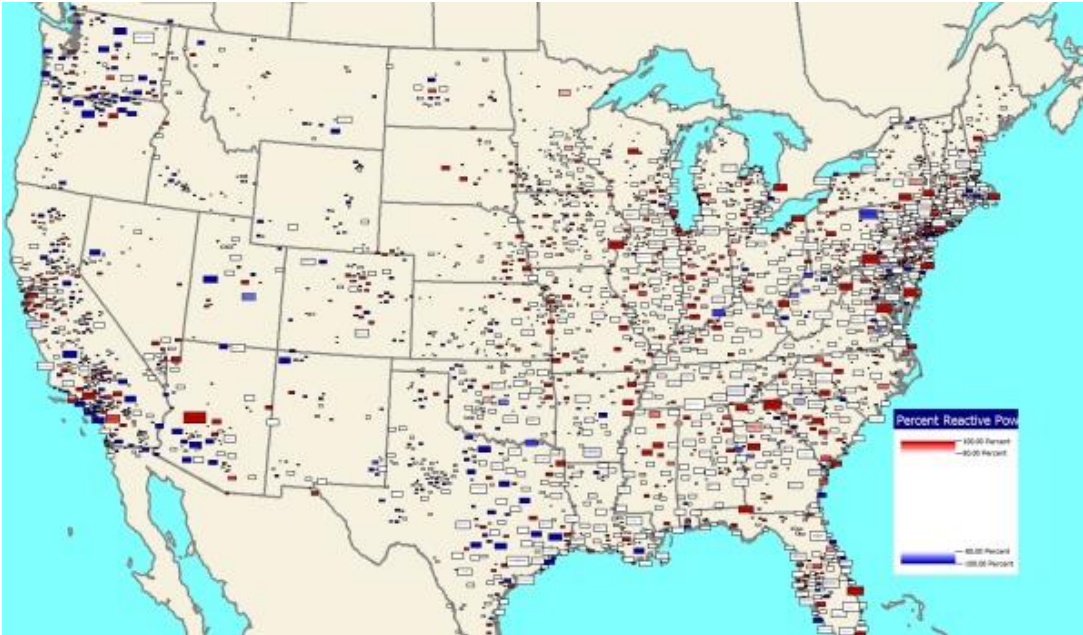


Figure 4.4 82,000 Bus Substation GDVs with Layout

4.4 GDV Summary Objects

However even with layout sometimes there are just too many GDVs to effectively display. In such situations the use of GDV summary objects can be helpful. These GDVs may be derived from summary objects already existing in the electric grid model, such as the areas shown in Figure 4.2, or may be dynamically determined. One quick approach is to just group the electric grid objects geographically and show the summary GDVs based upon an xy grid covering the entire system footprint. Such summaries could be used with actual values or with the previously mentioned differences between solutions. As an example, Figure 4.5 uses a 25 by 15 grid of GDV summary objects to show the change in the generation during a time-domain study on the 82K bus system. The initial contingency is the loss of about 2800 MW of generation in the Southwest U.S and the 60 Hz system response is integrated using a $\frac{1}{4}$ cycle time step. The size of each GDV is proportional to the change in generation while its fill color is set to red where generation is lost, and blue where it is increased. The figure shows data for four seconds after the contingency. This use of the GDVs summaries allows the system generator change pattern to be quickly determined.

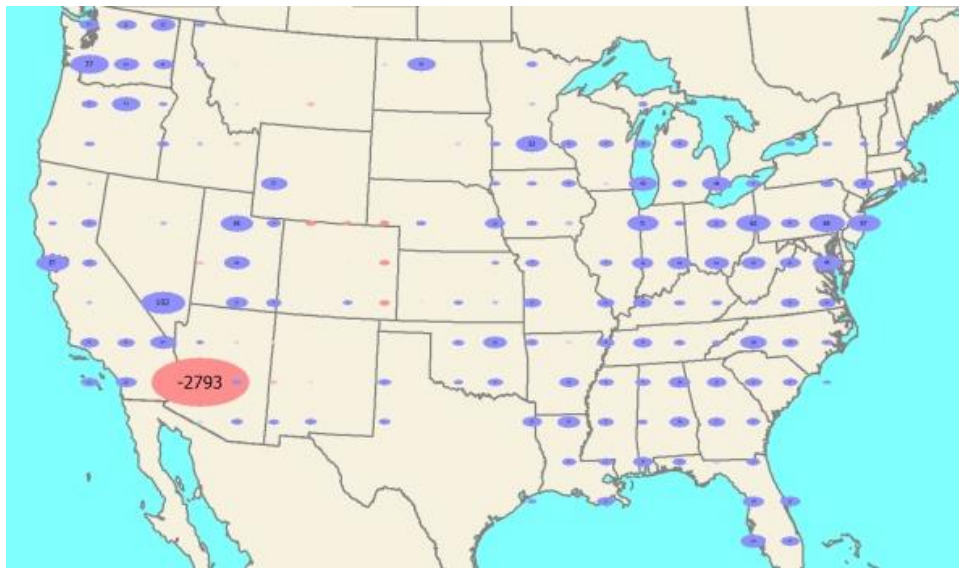


Figure 4.5 82K System Generation Summary Objects using a 25 by 15 Grid

This concept can be extended to show the overall flow pattern of electricity in a grid. The challenge with summarizing branch flows for large systems is just the sheer number of branches (e.g., Figure 4.1). Techniques such as using flow arrows [43] changing the thickness of the individual lines on the oneline [52] can be used for smaller systems, but have difficulty in scaling to extremely large systems. A newer technique from [53] visualizes electric grid flows as a vector field can be scaled to larger systems. Complementing these approaches, GDV flow summary objects can be defined using the same xy grid approach as the regular summary object. Each of these flow objects can be configured to show the flow entering or exiting the summary object in the four different directions associated with the underlying grid. The amount of flow can be visualized by changing the thickness of the line's joining the neighboring flow objects and/or its color; arrows are superimposed on the lines to show the direction of flow. Figure 4.6 shows an example for the 82K system in which the system is partitioned into a 16 by 8 grid. At each grid location, a regular GDV

summary object is also added, showing the net real power injection (with yellow for generation, magenta for load).

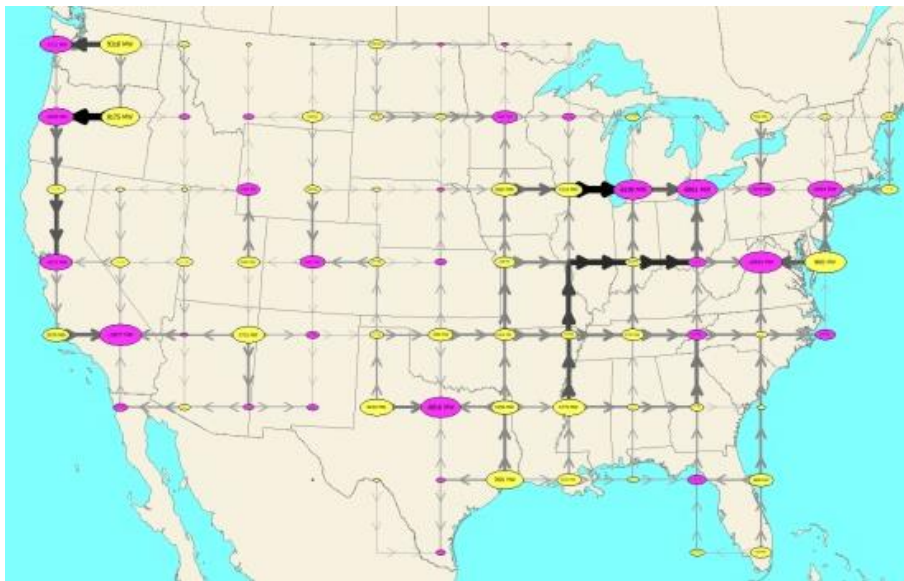


Figure 4.6 82K Substation Flow Visualization with Aggregate Line Flows (16 by 8 Grid)

In calculating the summary flow, the impact of lines that both terminate in the summary location and pass through the location without terminating (such as a longer high voltage line) are considered. As with all GDVs, the objects can visualize either actual values or the difference in flows from some base case. Given the aggregate nature of these summaries, the inclusion of a geographic background might be less useful, Figure 4.7 shows the Figure 4.6 results except 1) the xy grid size is increased to 28 by 16, 2) the background and injection symbols are removed, and 3) the color scale was changed. Such displays could be most useful in allowing for quick comparisons of different operating conditions.

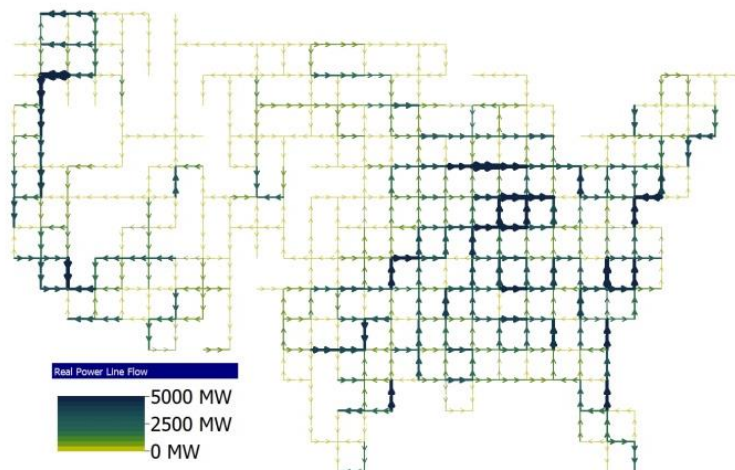


Figure 4.7 82K Substation Flow Visualization with Aggregate Line Flows (28 by 16 Grid)

5. Concluding Remarks

This project aimed to highlight the key issues that may need to be considered in assessing the ac interconnection of the North American Eastern and Western Interconnection grids, with a focus on the dynamic aspects. To protect confidential information about the real grids, realistic but fictitious synthetic grids were used to demonstrate the methodology. These grids cover the same geographic footprints as the real ones, use real generation information as it is publicly available and mimic load distribution from census data, but the transmission lines are entirely fictitious.

The methodology involved first overcoming challenges associated with combining actual detailed WECC and EI models and second making the actual connections between the east and west systems with ac ties. These include the ability to handle very large systems with overlapping bus and area numbers; determining the location, number and types of connections needed for a reasonable steady state and dynamic performance of the combined system; initializing tie flows for studies, etc. Then after assigning appropriate impedances and ratings, a few static power flow studies are performed to determine distribution of flows across each tie, and estimate the MW transfer capability. The goal of these studies is to demonstrate methods to pinpoint the heavier loaded ties and locations where modest upgrades could lead to major improvement in transfer capability.

Next, the main part of the project i.e. dynamic assessments of the interconnection involved a wide variety of dynamic simulations of the systems. The key limiting characteristic on interconnecting the EI and WI is that during generator loss contingencies in the WI, approximately 75 to 80% of the lost power will flow through the Interface from east to west. This is due to the governor response that takes place uniformly through the interconnect and most of the generation is east of the Interface. This issue is fundamental to interconnecting large grids and does require any interface joining two such larger grids be able to handle this flow (at least until AGC can respond). In particular for the EI and WECC, there need to be more than just a few tielines. For the flow to return to pre-contingency values, AGC needs to be modeled in these simulations, which is not a common practice. To address this, AGC was implemented and included in our dynamic simulations run for several minutes. In the scenarios run both for the real and synthetic interconnections, the grids were stable when AGC response was considered.

A major challenge associated with these analyses was understanding what is occurring in the large scale electric grids, particularly when they could be subject to unusual operating conditions such as those associated with a new ac interconnection. This in addition to the large quantity of simulation results, especially dynamics with hundreds of thousands of buses, models, states, etc. To this end, geographic data views (GDV), which are electric grid display objects whose location is dynamically determined from geographic information embedded in an electric grid model, were developed and used extensively. Different examples of GDV's and how they can meaningfully convey a large amount of key information were shown.

The studies shown in this report are not meant to be all-encompassing and covering all possible conditions and scenarios. Rather, these are preliminary studies performed to illustrate issues associated with the interconnection of large-scale grids, with an eye towards providing a test system for other researchers. These grids i.e. the individual synthetic east and west and their ac

interconnected versions are available publicly for researchers to access and run their own scenarios in addition to those shown in this report. This may include, 1) different ac tie connections, 2) static and dynamic contingency scenarios, 3) loading conditions, 4) renewable generation, 5) time series simulations such as those used in OPFs, and so on.

References

- [1] J. Cohn, “When the grid was the grid: the history of North America’s brief coast-to-coast interconnected machine [scanning our past],” *Proceedings of the IEEE*, vol. 107, no. 1, pp. 232–243, 2019.
- [2] N. Cohn, S. B. Biddle, R. G. Lex, E. H. Preston, C. W. Ross, and D. R. Whitten, “On-line computer applications in the electric power industry,” *Proceedings of the IEEE*, vol. 58, no. 1, pp. 78–87, 1970.
- [3] I. Toljan, E. Banovac, and S. Tešnjač, “Development of UCTE and Reconnection of 1st and 2nd Pan-European Synchronous Zones,” in *Proceedings of the 4th IASME/WSEAS international conference on Energy & environment. World Scientific and Engineering Academy and Society (WSEAS)*, 2009, pp. 419–424.
- [4] H. Breulmann, E. Grebe, M. Löising et al., “Analysis and damping of inter-area oscillations in the UCTE/CENTREL power system,” *CIGRE Session*, no. 38-113, 2000.
- [5] M. Luther, I. Biernacka, D. Preotescu et al., “Feasibility Aspects of a Synchronous Coupling of the IPS/UPS with the UCTE,” *CIGRE Session*, no. C1 204, 2010.
- [6] S. S. Lee, J. K. Park, and S. I. Moon, “Power system interconnection scenario and analysis between Korean peninsula and Japan,” in *2003 IEEE Power Engineering Society General Meeting (IEEE Cat. No.03CH37491)*, vol. 3, 2003, pp. 1455–1460 Vol. 3.
- [7] Z. Xu, H. Dong, and H. Huang, “Debates on ultra-high-voltage synchronous power grid: the future super grid in China?” *IET Generation, Transmission Distribution*, vol. 9, no. 8, pp. 740–747, 2015.
- [8] A. L. Figueroa-Acevedo, “Opportunities and benefits for increasing transmission capacity between the US eastern and western interconnections,” PhD Dissertation, Iowa State University, 2017.
- [9] Y. Li and J. D. McCalley, “Design of a High Capacity Inter-Regional Transmission Overlay for the U.S.” *IEEE Transactions on Power Systems*, vol. 30, no. 1, pp. 513–521, 2015.
- [10] M. A. Elizondo, N. Mohan, J. O’Brien, Q. Huang, D. Orser, W. Hess, H. Brown, W. Zhu, D. Chandrashekhara, Y. V. Makarov, D. Osborn, J. Feltes, H. Kirkham, D. Duebner, and Z. Huang, “HVDC macrogrid modeling for power-flow and transient stability studies in North American continental-level interconnections,” *CSEE Journal of Power and Energy Systems*, vol. 3, no. 4, pp. 390–398, 2017.
- [11] A. Bloom (National Renewable Energy Laboratory), “Interconnection Seams Study,” in *TransGrid-X 2030 Symposium*, Ames, Iowa, 2018.
- [12] Western Area Power Administration, “East/West AC Intertie Feasibility Study,” Tech. Report, 1994.
- [13] J. Caspary, J. McCalley, S. Sanders, and M. Stoltz, “Proposed Eastern Interconnection and Western Electricity Coordinating Council Seams Study,” in *CIGRE US National Committee 2015 Grid of the Future Symposium*, 2015, pp. 1–11.
- [14] A. B. Birchfield, T. Xu, K. M. Gegner, K. S. Shetye, and T. J. Overbye, “Grid structural characteristics as validation criteria for synthetic networks,” *IEEE Transactions on Power Systems*, vol. 32, no. 4, pp. 3258–3265, July 2017.

- [15] T. Xu, A.B. Birchfield, T.J. Overbye, "Modeling, Tuning and Validating System Dynamics in Synthetic Electric Grids," *IEEE Transactions on Power Systems*, vol. 33, pp. 6501-6509, November 2018.
- [16] <https://electricgrids.engr.tamu.edu/>
- [17] IEEE PES Power System Dynamic Performance Committee, "Stability definitions and characterization of dynamic behavior in systems with high penetration of power electronic interfaced technologies, PES-TR77, April 2020.
- [18] P. Kundur, J. Paserba, V. Ajjarapu, G. Andersson, A. Bose, C. Canizares, N. Hatziargyriou, D. Hill, A. Stankovic, C. Taylor, T. Van Cutsem, V. Vittal, "Definition and classification of power system stability IEEE/CIGRE joint task force on stability terms and definitions," *IEEE Transactions on Power Systems*, Vol. 19, no. 3, pp. 1387–1401, Aug 2004.
- [19] M. Crow and J. G. Chen, "The multirate method for simulation of power system dynamics," *IEEE Transactions on Power Systems*, vol. 9, no. 3, p. 1684–1690, August 1994.
- [20] J.H. Yeo, W.C. Trinh, W. Jang, T.J. Overbye, "Assessment of Multirate Methods for Power System Dynamics Analysis," accepted for *2020 North American Power Symposium*, Tempe, AZ, April 2021.
- [21] M.S. Dyrkacz, C.C. Young, F.J. Maginniss, "A Digital Transient Stability Program Including the Effects of Regulator, Exciter and Governor Response," *Trans. AIEE, Part III: Power Apparatus and Systems*, pp. 1245-1254, February 1961.
- [22] T.J. Overbye, J.L. Wert, K.S. Shetye, F. Safdarian, A. B. Birchfield, "The Use of Geographic Data Views to Help With Wide-Area Electric Grid Situational Awareness," Submitted to *Texas Power and Energy Conference (TPEC) 2021*, Feb. 2021.
- [23] T.J. Overbye, K.S. Shetye, J.L. Wert, Wei Trinh, A.B. Birchfield, T. Rolstad, J.D. Weber, "Techniques for Maintaining Situational Awareness During Large-Scale Electric Grid Simulations," Submitted to *Power and Energy Conference at Illinois (PECI) 2021*, Apr. 2021, Champaign, IL.
- [24] W. Trinh, K.S. Shetye, I. Idehen, T.J. Overbye, "Iterative Matrix Pencil Method for Power System Modal Analysis," Proc. 52nd Hawaii International Conference on System Sciences, Wailea, HI, January 2019
- [25] I. Idehen, B. Wang, K.S. Shetye, T.J. Overbye, J.D. Weber, "Visualization of Large-Scale Electric Grid Oscillation Modes," Proc. 2018 North American Power Symposium, Fargo, ND, September 2018
- [26] U.S Canada Power System Outage Task Force, Final Report on the August 14, 2003 Blackout in the United States and Canada, April 2004.
- [27] M.R. Endsley, "Toward a theory of situation awareness in dynamic systems," *Human Factors*, Vol. 37, pp. 32-64, March 1995.
- [28] C.L. Wickens, "Situation Awareness: Review of Mica Endsley's 1995 Articles on Situation Awareness Theory and Measurement," *Human Factors*, Vol. 50, pp. 397-403, June 2008.
- [29] C. Basu, M. Padmanaban, S. Guillon, L. Cauchon, M. De Montigny, I. Kamwa, "Situational awareness for the electric power grid," *IBM Journal of Research and Development*, Vol. 60, Issue 1, 2016.
- [30] J. Wu, K. Ota, M. Dong, J. Li, H. Wang, "Big Data Analysis-Based Security Situational Awareness for Smart Grid," *IEEE Trans. Big Data*, Vol. 4, pp. 408-417, July-Sept. 2018.

- [31] Y. Liu, W. Yao, D. Zhou, L. Wu, S. You, H. Liu, L. Zhan, J. Zhao, H. Lu, G. Gao, Y. Liu, "Recent Development of FNET/GridEye – A Situational Awareness Tool for Smart Grid," *CSEE Journal of Power and Energy Systems*, Vol. 2, pp. 19-27, Sept. 2016.
- [32] The National Research Council, "Modeling Human and Organizational Behavior," *The National Academies Press*, Washington DC, 1998.
- [33] T.J. Overbye, T.R. Hutchins, K.S. Shetye, J. Weber, S. Dahman, "Integration of Geomagnetic Disturbance Modeling into the Power Flow: A Methodology for Large-Scale System Studies," *Proc. 2012 North American Power Symposium*, Champaign, IL, September, 2012
- [34] J. D. Weber and T. J. Overbye, "Voltage contours for power system visualization," *IEEE Trans. on Power Systems*, Vol. 15, pp. 404-409, February, 2000.
- [35] P.C. Wong, K. Schneider, P. Mackey, H. Foote, G. Chin, R. Guttromson, J. Thomas, "A Novel Visualization Technique for Electric Grid Power Analytics," *IEEE Trans. Visualization and Computer Graphics*, Vol. 15, pp. 410-423, May/June 2009.
- [36] T.J. Overbye, J.D. Weber, "Smart Grid Wide-Area Transmission System Visualization," *Engineering, Chinese Academy of Engineering*, vol. 1, December 2015, pp. 466-474. Available online at <http://engineering.org.cn/EN/10.15302/J-ENG-2015098>.
- [37] P. Cuffe, A. Keane, "Visualizing the Electrical Structure of Power Systems," *IEEE Systems Journal*, Vol. 11, pp. 1810-1821, Sept. 2017.
- [38] A.L. Figueroa-Acevedo, C-H. Tsai, K. Gruchalla, Z. Claes, S. Foley, J. Bakke, J. Okullo, A.J. Prabhakar, "Visualizing the Impacts of Renewable Energy Growth in the U.S. Midcontinent," *IEEE Open Access Journal of Power and Energy*, Vol. 7, pp. 91-99, Jan. 2020.
- [39] T.J. Overbye, E.M. Rantanen, S. Judd, "Electric power control center visualizations using geographic data views," *Bulk Power System Dynamics and Control -- VII. Revitalizing Operational Reliability -- 2007 IREP Symposium*, Charleston, SC, August 2007, pp1-8.
- [40] T.J. Overbye, "Wide-area power system visualization with geographic data views," *Proc. 2008 IEEE PES General Meeting*, Pittsburgh, PA, July 2008.
- [41] A.B. Birchfield, K.M. Gegner, T. Xu, K.S. Shetye, T.J. Overbye, "Statistical Considerations in the Creation of Realistic Synthetic Power Grids for Geomagnetic Disturbance Studies," *IEEE Transactions on Power Systems*, vol. 32, pp. 1502-1510, March 2017.
- [42] A.B. Birchfield, T. Xu, T.J. Overbye, "Power Flow Convergence and Reactive Power Planning in the Creation of Large Synthetic Grids," *IEEE Transactions on Power Systems*, vol. 33, pp. 6667-6674, November 2018.
- [43] T.J. Overbye, J.D. Weber, "Visualization of Power System Data," *Proc. 33rd Hawaii International Conference on System Sciences*, Wailea, HI, Jan. 2000.
- [44] Glossary of Terms Used in NERC Reliability Standards, NERC, June 2020, online at www.nerc.com/files/glossary_of_terms.pdf.
- [45] T.J. Overbye, J. Wert, A.B. Birchfield, J.D. Weber, "Wide-Area Electric Grid Visualization Using Pseudo-Geographic Mosaic Displays," *Proc. 2019 North American Power Symposium*, Wichita, KS, October 2019.
- [46] A.B. Birchfield, T.J. Overbye, "Mosaic Packing to Visualize Large-Scale Electric Grid Data," *IEEE Open Access Journal of Power and Energy*, Vol. 7, pp. 212-221, June 2020.

- [47] P. Eades, "A Heuristic for Graph Drawing", *Congressus Numerantium*, Vol. 42, pp. 149–160, 1984.
- [48] S.C. Teja and P.K. Yemula, "Power network layout generation using force-directed graph technique," in *Proc. 18th Nat. Power Syst. Conf.*, Guwahati, India, 2014.
- [49] A. de Assis Mota, L.T.M. Mota, "Drawing meshed one-line diagrams of electric power systems using a modified controlled spring embedder algorithm enhanced with geospatial data," *Journal of Computer Science*, Vol. 7, no. 2, pp. 234-241, 2011.
- [50] A.B. Birchfield, T.J. Overbye, "Techniques for Drawing Geographic One-line Diagrams: Substation Spacing and Line Routing," *IEEE Transactions on Power Systems*, vol. 33, pp. 7269-7276, November 2018.
- [51] C. Ware, *Information Visualization: Perception for Design*, Fourth Edition, Morgan Kaufmann, 2021.
- [52] P.M. Mahadev, R.D. Christie, "Envisioning Power System Data: Concepts and a Prototype System State Representation," *IEEE Trans. on Power Systems*, Vol. 8, pp. 1084-1090, August 1993.
- [53] S. Molnar, K. Gruchalla, "Visualizing Electric Power Systems as Flow Fields," *Workshop of Visualization in Environmental Sciences*, Brno, Czech Republic, June 2018.